

**Analysis of Hydrodynamic,  
Thermal and Salinity Effects  
of Deep Injection of Residual  
Water at the AOSTRA  
Underground Test Facility**

**Prepared for  
Conservation and Protection,  
Environment Canada**

**by**

**Stefan Bachu  
J.R. Underschultz  
L.P. Yuan**

**Alberta Geological Survey  
Alberta Research Council**

**March 31, 1994**

## **DISCLAIMER**

This report was prepared as an account of work sponsored by the Alberta Research Council and Environment Canada, Conservation and Protection. Every possible effort was made to ensure that the work conforms to accepted scientific practice. However, neither the Alberta Research Council (ARC), nor any of its employees, makes any warranty, express or implied, or assumes any legal liability or responsibility for the accuracy, completeness, or usefulness of any information, product, or process disclosed, or represents that its use would not infringe privately owned rights. Reference herein to any specific commercial product, process, or service by trade name, trademark, manufacturer, or otherwise, does not necessarily constitute or imply its endorsement, recommendation, or favouring by the ARC. The views and opinions of the authors expressed herein do not necessarily state or reflect those of the ARC.

**TABLE OF CONTENTS**

	<b><u>Page</u></b>
EXECUTIVE SUMMARY .....	5
INTRODUCTION .....	7
WABISKAW AQUIFER CHARACTERISTICS .....	12
GEOLOGY .....	12
HYDROGEOLOGY .....	14
ROCK PROPERTIES .....	17
Porosity .....	17
Permeability .....	23
Compressibility and Fracturing Threshold .....	24
EFFECTS OF INJECTION .....	25
MATHEMATICAL MODEL .....	27
Fluid Flow .....	27
Solute Transport .....	34
Heat Transfer .....	36
Initial and Boundary Conditions .....	38
SIMULATION OF INJECTION .....	44
Hydrodynamic Effects .....	44
Thermal and Salinity Effects .....	48
CONCLUSIONS .....	57
REFERENCES .....	60

## LIST OF FIGURES

	<u>Page</u>
Figure 1. Location map of the UTF site in northeast Alberta . . . . .	8
Figure 2. Ground surface elevation map at the UTF site . . . . .	13
Figure 3. Isopach of the Wabiskaw aquifer . . . . .	15
Figure 4. Top structure elevation of the Wabiskaw aquifer . . . . .	16
Figure 5. Salinity distribution in the Wabiskaw aquifer . . . . .	18
Figure 6. Freshwater hydraulic-head distribution in the Wabiskaw aquifer . . . . .	19
Figure 7. Areal distribution of well-averaged porosity in the Wabiskaw aquifer . . . . .	21
Figure 8. Frequency distribution of well-averaged porosity in the Wabiskaw aquifer . . . . .	22
Figure 9. Forecasted injection rate at the UTF site (from AOSTRA, 1992) . . . . .	26
Figure 10. Plan view of the finite element grid used in numerical simulations of injection . . . . .	30
Figure 11. Calculated hydraulic-head buildup in the Wabiskaw aquifer at the injection node using the FE3DGW numerical model . . . . .	31
Figure 12. Calculated areal spread of the hydraulic-head (pressure) buildup in the Wabiskaw aquifer at the end of the injection period, using the FE3DGW numerical model . . . . .	32
Figure 13. Calculated (simulated) distribution of baseline freshwater hydraulic-head (m) in the Wabiskaw aquifer, using the CFEST numerical model . . . . .	43
Figure 14. Calculated hydraulic-head buildup at the injection node in the Wabiskaw aquifer, using the CFEST numerical model and assuming the same properties for injected and aquifer waters . . . . .	45

Figure 15.	Calculated areal spread of hydraulic-head buildup in the Wabiskaw aquifer at the end of the injection period, using the CFEST numerical model and assuming the same properties for injected and aquifer waters . . . . .	46
Figure 16.	Calculated hydraulic-head buildup at the injection node in the Wabiskaw aquifer, using the CFEST numerical model, for properties of injected water different from those of the aquifer water . . . . .	50
Figure 17.	Calculated areal spread of hydraulic-head buildup in the Wabiskaw aquifer at the end of the injection period, using the CFEST numerical model, for properties of injected water different from those of the aquifer water . . . . .	51
Figure 18.	Calculated temperature increase at the injection node in the Wabiskaw aquifer . . . . .	52
Figure 19.	Calculated salinity decrease at the injection node in the Wabiskaw aquifer . . . . .	54
Figure 20.	Calculated areal spread of the dilution plume in the Wabiskaw aquifer at the end of the injection period . . . . .	55

## EXECUTIVE SUMMARY

This report presents the results of a computer-based evaluation of hydrodynamic, thermal and salinity effects of deep injection of residual water in the Wabiskaw aquifer at the Underground Test Facility (UTF) operated by the Alberta Oil Sands Technology and Research Authority (AOSTRA). The evaluation is based on numerical simulations of injecting up to 900,000 m<sup>3</sup> of produced, blowdown and regeneration water over a period of two years. The salinity of the injected water is lower than that of formation water, while its temperature is higher. Thus, the main purpose of the evaluation is to assess to what extent the natural pressure, temperature and concentration fields in the Wabiskaw aquifer will be affected and modified by residual-water injection. This report is the result of a collaborative agreement between Environment Canada and the Alberta Research Council to study the hydrogeological effects of deep injection at the UTF site. AOSTRA's cooperation and support with data is gratefully acknowledged.

Mathematical and numerical modelling of coupled processes of fluid flow, heat transfer and mass (solute) transport in porous media was used in the present study to evaluate the hydrodynamic, thermal and salinity effects of deep injection in the Wabiskaw aquifer. In addition, the spatial variability in aquifer properties, particularly porosity, was taken into account. The porosity distribution was obtained from geophysical logs calibrated on core analyses, resulting in a better representation than that obtained previously from core analyses only. The numerical simulations, based on forecasted

rates of injection, indicate that the pressure buildup at the injection site will remain below the accepted limit of 90% of the rock-fracturing threshold. After cessation of injection, the pressure buildup will rapidly decay due to the high hydraulic diffusivity of the aquifer. The areal spread of pressure buildup will be asymmetric, reaching between 4 km in the northwest and 6 km in the southeast because of lower aquifer porosity southeast of the injection site. The temperature is not likely to increase significantly because of heat transfer from the injected water to the aquifer water and rock, and because of heat losses by conduction through the overlying and underlying aquitards. The thermal effects of injection are likely to be felt at no more than 400 m from the injection well. After cessation of injection, the temperature will slowly decay because of low thermal diffusivity of aquifer water and rocks. Because the salinity of the injected residual water is actually lower than that of aquifer water, a dilution plume will form as a result of injection. The dilution plume will be slightly asymmetric, at the end of the injection period reaching approximately 500 m northeast from the injection site, but only approximately 300 - 350 m in other directions. This asymmetry is attributed to the effect of the northeastward flow of aquifer water. After cessation of injection, the initial pressure regime in the aquifer will be rapidly re-established, and the dilution plume will be carried by the natural flow of aquifer water with a velocity estimated to be approximately 2.5 m/a. Thus, overall, the numerical simulations show that the injection of the proposed volume of residual water at the UTF site is not likely to have any significant hydrogeological effect in the Wabiskaw aquifer.

## INTRODUCTION

The economic success of enhanced oil recovery (EOR) operations depends, among other factors, on the environmentally safe and economically affordable management of produced water. In many cases some or all of the produced water is recycled. However, in most instances some residual water has to be disposed of. Deep well injection generally provides a cost effective, technically feasible and environmentally safe option for the disposal of residual water, and is a method preferred by the oil industry (CPA, 1990; Sadler, 1991). According to the Alberta Hazardous Chemicals Act, water produced in association with the recovery of oil, bitumen or gas, saline fluids, boiler blowdown water and neutralized caustic or acid water are not defined as hazardous. The regulatory agencies, Alberta Environmental Protection and the Alberta Energy Resources Conservation Board (ERCB), classify the injection/disposal well for such residual water as Class II, subject to various regulations for well completion, injection and monitoring. No restrictions on water quality are imposed for pilot operations in the Athabasca area (Nelson et al., 1991). With respect to injection conditions, the main requirement is that the injection pressure does not exceed 90% of the rock fracturing pressure.

The Alberta Oil Sands Technology and Research Authority (AOSTRA) is developing the Underground Test Facility (UTF) near Fort McMurray, Alberta (Figure 1) for the extraction of bitumen from the near-surface Athabasca oil sand deposit using a steam-assisted gravity drainage (SAGD) recovery process. During an initial two-year



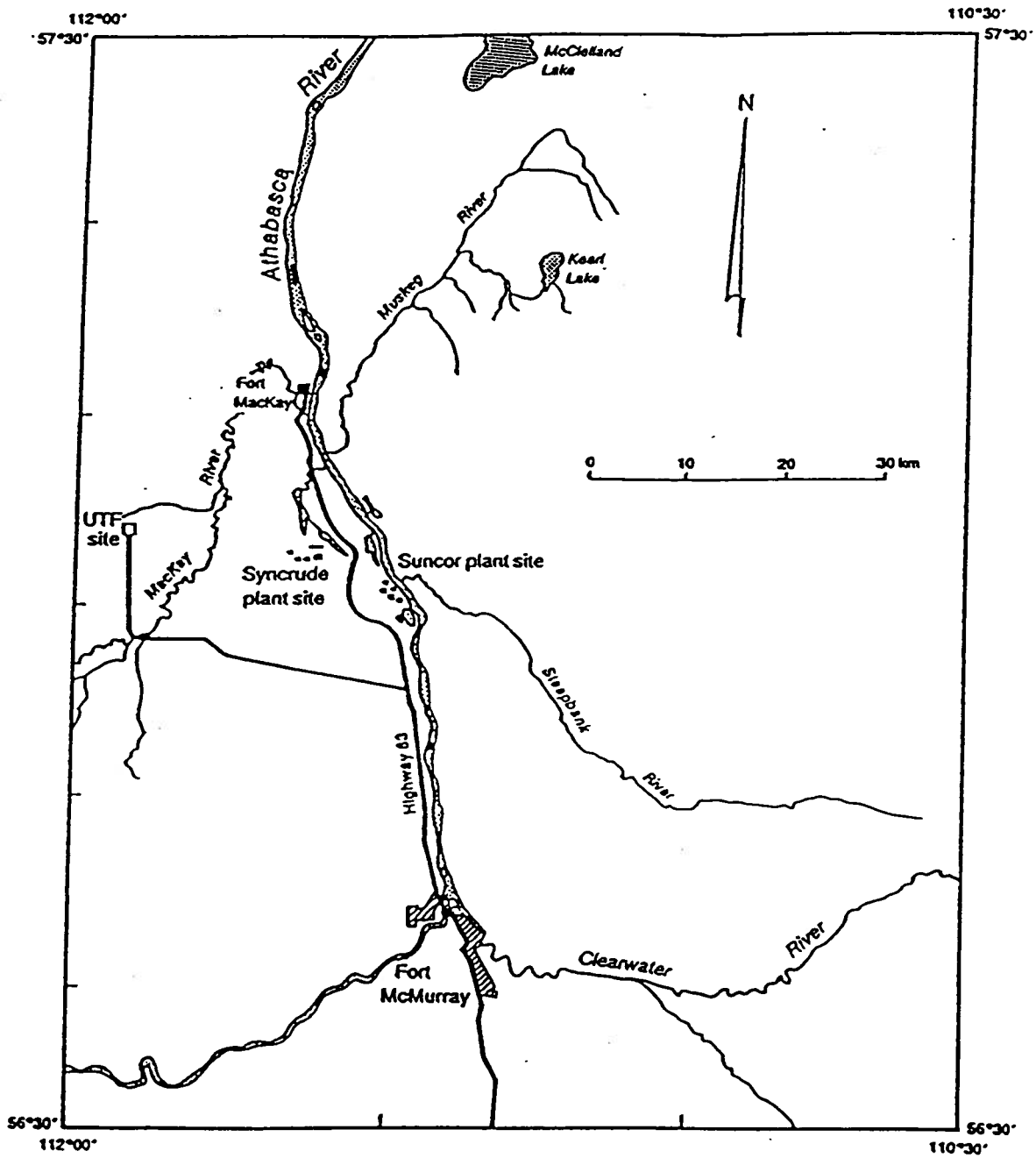


Figure 1: Location map of the UTF site in northeast Alberta.

expansion period, AOSTRA plans to dispose of 900,000 m<sup>3</sup> of residual water by injecting it into the sands of the Wabiskaw Member of the Clearwater Formation (Mannville Group). An initial study identified several geological formations as potential disposal units. In ascending stratigraphic order from the crystalline Precambrian basement, these formations are: Granite Wash, Winnipeagons Fm., Slave Point Fm., the Calumet and Moberly members of the Waterways Fm., McMurray Fm. basal water sands, and Wabiskaw Member sands of the Clearwater Fm. Of these, only the Wabiskaw Member was deemed to be suitable for injecting the planned volume of residual water (AOSTRA, 1992). This conclusion was subsequently confirmed by the hydrogeological analysis of the deep aquifers at the UTF site and by numerical modelling of geochemical and hydrodynamic effects of injecting residual water into these aquifers (Petroleum Geoscience Section, 1993).

The Basal (Granite Wash) aquifer is very thin and of very low porosity and permeability caused by sand cementation (AOSTRA, 1992). The carbonate Winnipegosis aquifer is plugged with salt originating from the overlying Prairie Formation salt deposits. Because of particularly low permeability, the pressure buildup at the injection well will probably rapidly reach the rock fracturing threshold (Petroleum Geoscience Section, 1993). In addition, this aquifer has a high potential for plugging by silica, dolomite and calcite precipitation as a result of injection (Petroleum Geoscience Section, 1993). Similar conclusions were reached with regard to the limestone aquifers (Slave Point and Calumet) of the Beaverhill Lake Group (Petroleum Geoscience Section, 1993). The

limestone Moberly aquifer is not suitable for injection mainly because it hosts the tunnels and access shafts of the UTF. The basal water sands of the McMurray Formation are unsuitable for deep injection of residual water because of their limited volume, hydraulic continuity with the underlying Moberly aquifer, and the existence of possible flow paths along the sub-Cretaceous unconformity toward discharge areas at the Athabasca River valley. The Wabiskaw aquifer has high porosity (around 30% on average) and high permeability (around 2 - 4 darcies on average). As a result, it is projected that the pressure induced by injection will rapidly diffuse away and the pressure buildup during injection will most probably remain significantly below the fracturing threshold estimated to be 2370 kPa (Petroleum Geoscience Section, 1993). From a geochemical point of view, the Wabiskaw aquifer is the most suitable for injection because of the low potential and rate for mineral precipitation. Because of very low temperature kinetics of silica and dolomite precipitation, it is expected that mineral precipitation, if any, will occur far from the injection well and will not significantly alter the hydraulic properties of the Wabiskaw aquifer (Petroleum Geoscience Section, 1993).

The preliminary evaluation of geochemical and hydrodynamic effects of deep injection of residual water at the UTF site (Petroleum Geoscience Section, 1993) consisted of numerical simulations based on average values for rock properties like porosity and permeability. The simulations took into account only hydrodynamic effects (fluid flow), without considering the fact that the injected water has a higher temperature and a lower salinity than the formation water. The previous preliminary study, while

confirming AOSTRA's decision to dispose of residual water in the Wabiskaw aquifer, concluded with the recommendation to model the effects of injection by taking into account the spatial variability in rock properties and the differences in temperature and salinity between the injected and formation waters. The present study attempts to account for this variability in evaluating the effects of deep injection of residual water at the UTF site. The study is the result of a collaborative program between the Alberta Research Council and Environment Canada, whose participation is gratefully acknowledged. The authors also wish to thank AOSTRA for its cooperation and data support.

## **WABISKAW AQUIFER CHARACTERISTICS**

### **GEOLOGY**

The sedimentary succession at the UTF site can be broadly divided into Paleozoic passive-margin strata and Cretaceous foreland-basin strata, separated by the sub-Cretaceous angular unconformity. The Paleozoic strata consist of the evaporite and carbonate dominated Elk Point and Beaverhill Lake groups, with the latter subcropping at the sub-Cretaceous unconformity. The Cretaceous strata consist only of the siliciclastic Mannville Group, with younger strata having been completely removed by erosion. A veneer of Pleistocene-age drift and other sediments of recent geological age, comprised primarily of unconsolidated sands and gravels, covers the bedrock. The UTF is located on relatively high ground between the valleys of the MacKay and Dover rivers which flow northeastward and discharge into the Athabasca River (Figure 2).

The Mannville Group strata generally consist of interbedded siliciclastics comprised of sand, shale and silt. Stratigraphically, the Mannville Group can be subdivided, in ascending order, into the McMurray, Clearwater and Grand Rapids formations. In the study area, the unconsolidated sands of the McMurray Formation are generally bitumen saturated. The Wabiskaw Member of the Clearwater Formation disconformably overlies the McMurray Formation, and can be subdivided into four units. The lowermost one is a basal erosional channel consisting of two localized bitumen-saturated sandy deposits.

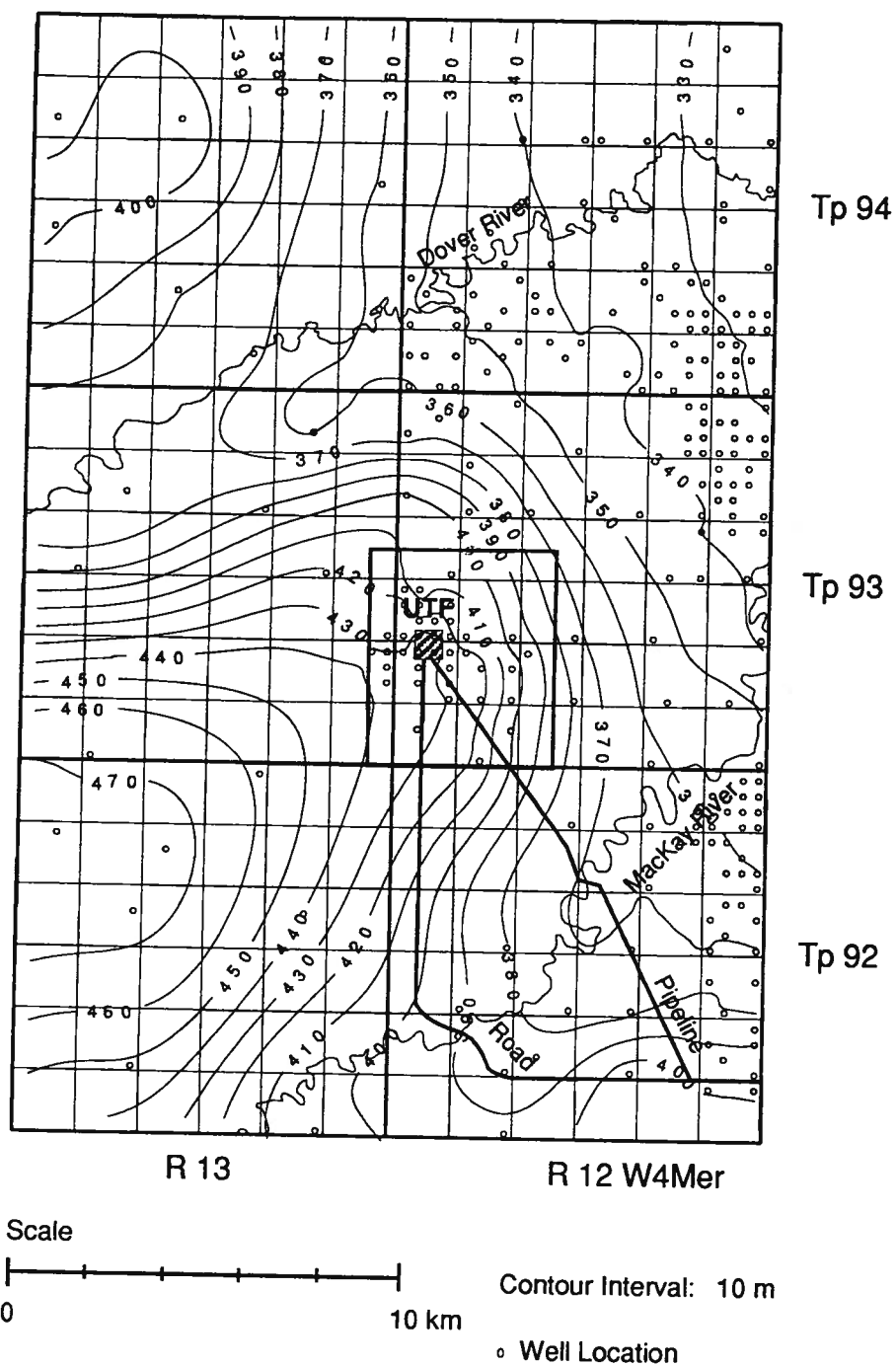


Figure 2: Ground surface elevation map at the UTF site.

Above them there is a wedge of sandy shale, named the lower shale wedge, which thickens and becomes progressively shaley to the southwest. Overlying this shale wedge is an upward coarsening, bioturbated sand which thins gradually from southwest to northeast. This sand forms the Wabiskaw aquifer. It varies in thickness from 2 to 16 m in the area around the UTF site (Figure 3). The structure top of the Wabiskaw aquifer is shown in Figure 4. A uniformly thick, black, often sandy/silty shale, overlies the upper sand. This confining upper marine shale defines the top of the Wabiskaw Member within the Clearwater Formation. Above the Wabiskaw Member, the remainder of the Clearwater Formation consists mainly of shale interbedded with thin, very fine-grained sand and silt. A relatively thick shale overlies the Wabiskaw Member, followed by two stacked coarsening-upward cycles, each grading from shale at the base to very fine sand or silt at the top. Each cycle is capped by a shale layer. The Clearwater Formation is conformably overlain in places by the Grand Rapids Formation, which consists of sands interbedded with shales.

## HYDROGEOLOGY

The bitumen-free Wabiskaw sands form an aquifer confined by the underlying McMurray-Wabiskaw and the overlying Clearwater-Wabiskaw shaley aquitards (Petroleum Geoscience Section, 1993). Very few formation water analyses and drillstem tests are available for the Wabiskaw aquifer in the vicinity of the UTF site (local scale).

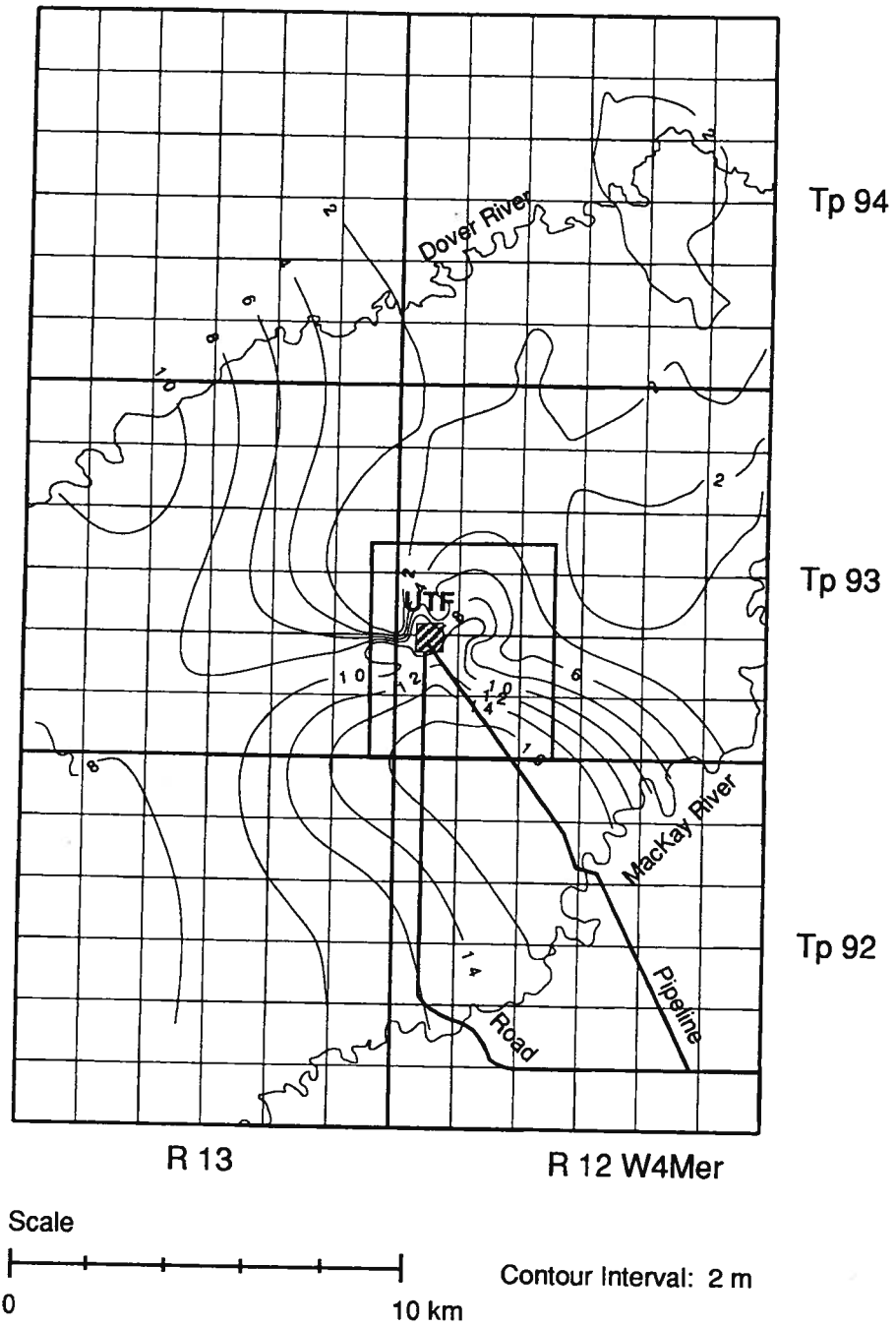


Figure 3: Isopach of the Wabiskaw aquifer.



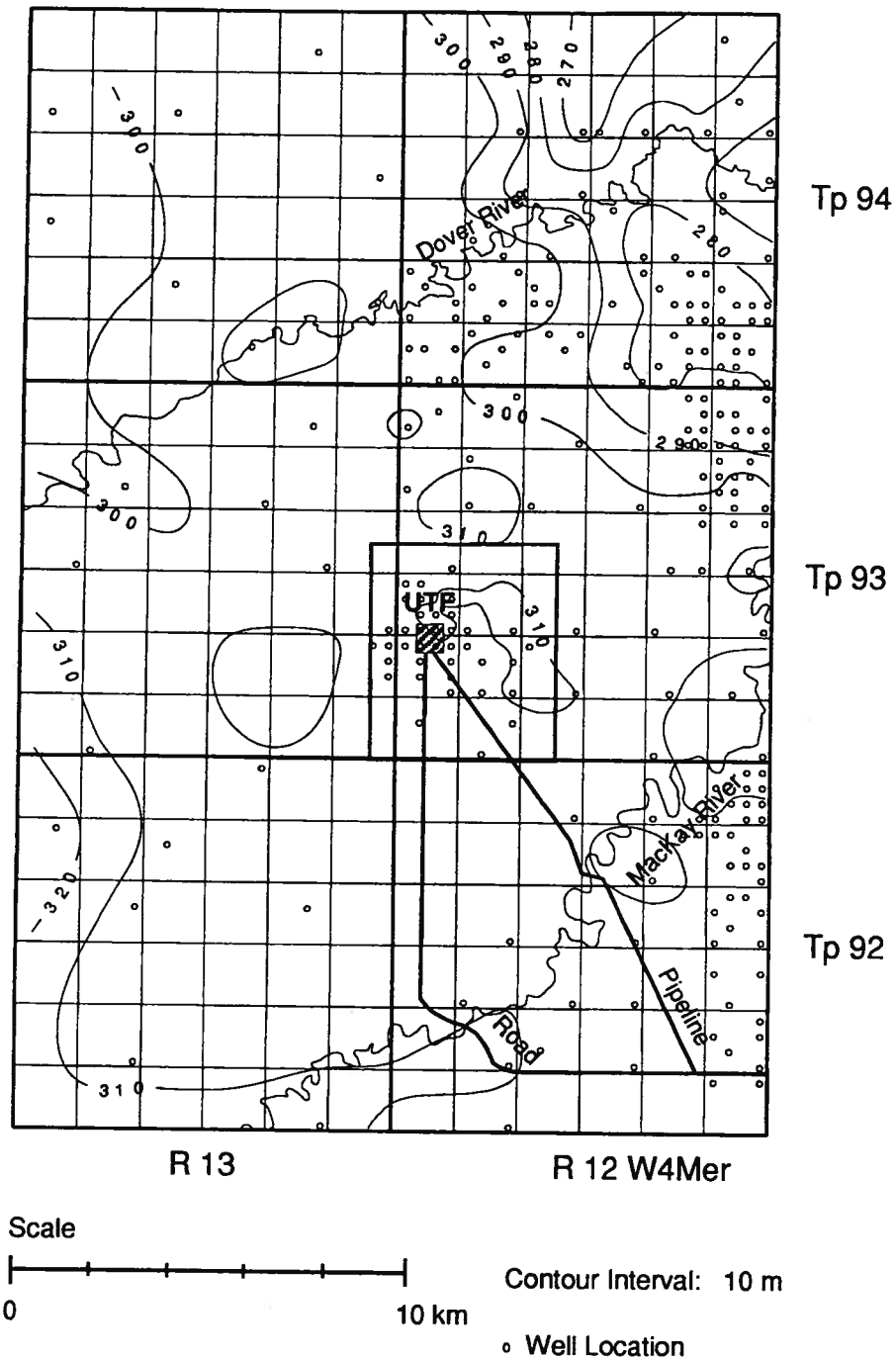


Figure 4: Top structure elevation of the Wabiskaw aquifer.

Salinity and pressure distributions (expressed as hydraulic heads) were obtained for the Wabiskaw aquifer from a previous, larger scale hydrogeological study (Petroleum Geology and Basin Analysis Group, 1992). The formation water is relatively fresh, with salinities in the 12,000 mg/l range (Figure 5). The potentiometric surface (Figure 6) for the Wabiskaw aquifer indicates that the formation waters flow in a local system from recharge in areas of relatively high topography in the southwest to discharge areas along the valleys of the MacKay and Athabasca rivers in the northeast.

## **ROCK PROPERTIES**

From the point of view of deep injection, the most important aquifer characteristics are porosity, permeability, compressibility and fracturing threshold. The most commonly determined parameter is porosity, obtained either from core measurements or from geophysical logs. Permeability could be measured at the plug scale in core samples, or directly at the well scale in drillstem tests. Rock compressibility and fracturing threshold are very seldom measured. However, AOSTRA has completed geotechnical testing at the UTF site.

### **Porosity**

Core samples were taken from Wabiskaw sand and porosity measured in 44 wells in the local study area defined by Tp. 92-94, R12-13, W4Mer. The average well-scale

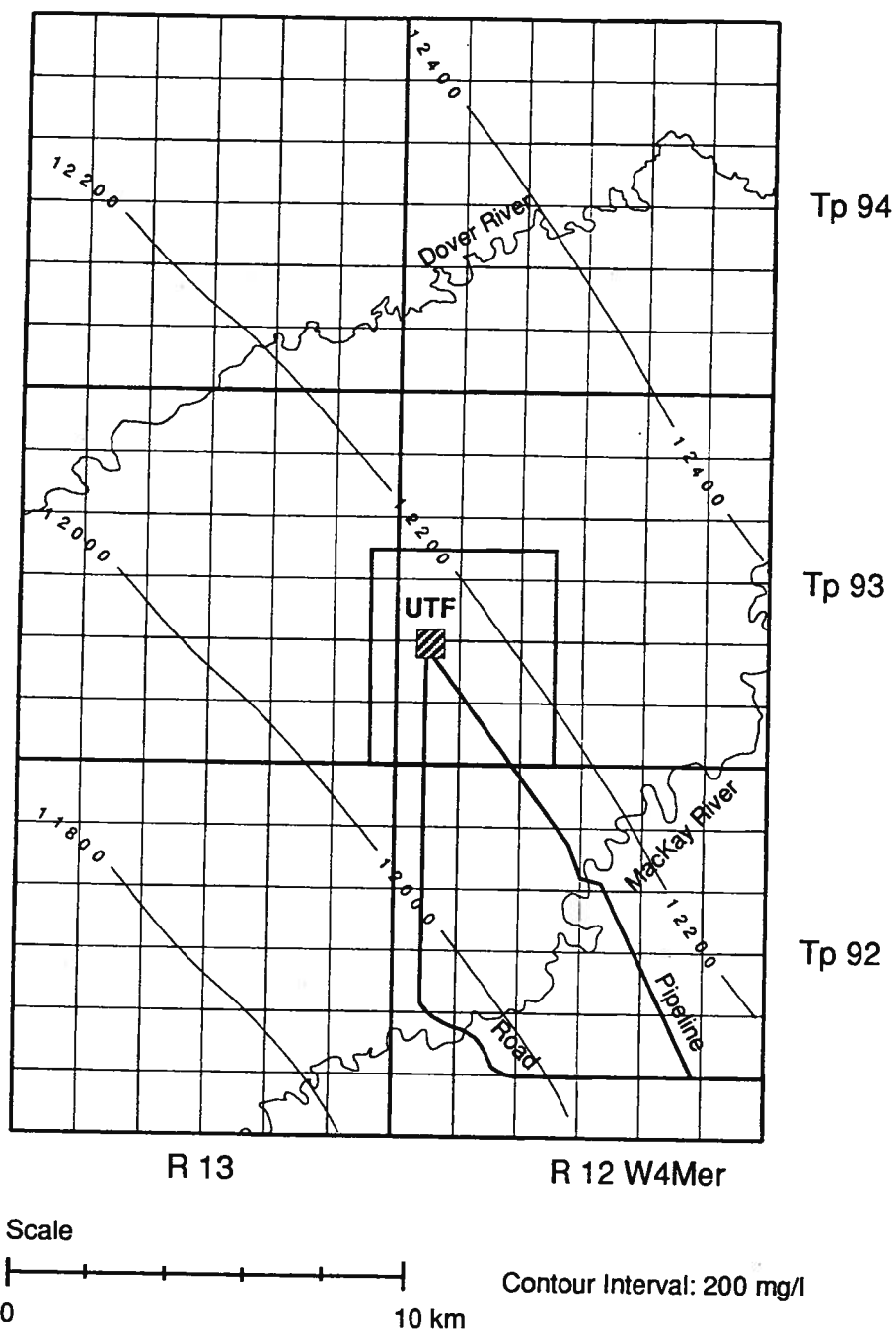


Figure 5: Salinity distribution (mg/l) in the Wabiskaw aquifer.

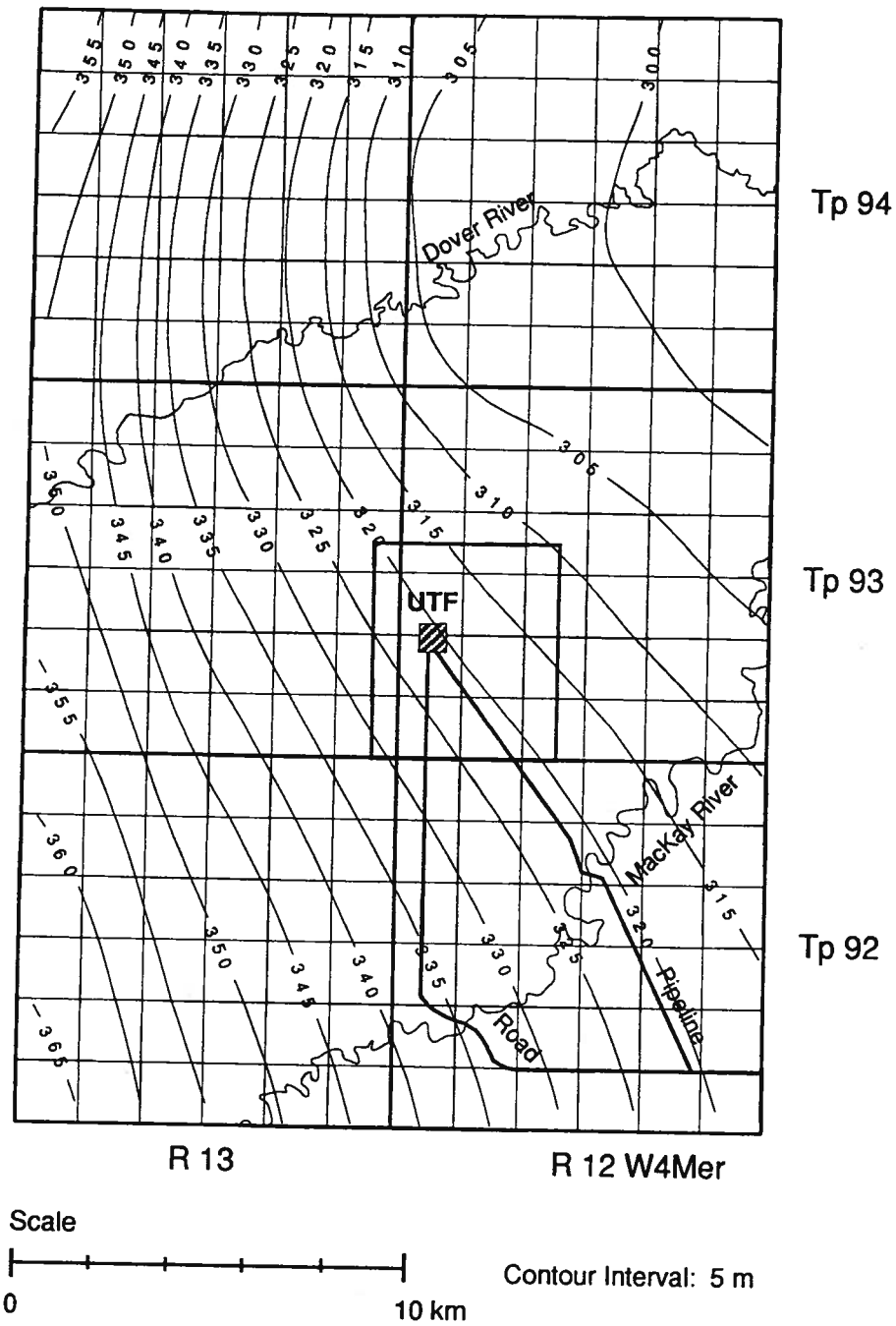


Figure 6: Freshwater hydraulic-head distribution (m) in the Wabiskaw aquifer.

porosity resulting from these measurements is 31% (Petroleum Geoscience Section, 1993). However, it is well known that core sampling has a tendency to be biased toward the clean, porous and permeable zones, thus leading sometimes to overestimates of rock properties. The Wabiskaw aquifer contains thin shaley interbedded layers which have the effect of decreasing the well and formation scale porosity and permeability. In order to circumvent the inherent bias in core sampling, well logs were used to estimate the porosity variation across the entire thickness of the Wabiskaw aquifer. The INTELLOG log analysis system was calibrated based on geophysical logs and porosity measurements taken from core within the same well. The geophysical logs not only ensured coverage of the entire aquifer thickness, but also increased the data base from 44 to 76 wells. Because porosity is an additive quantity, the well-scale value is obtained by weight-averaging the geophysical-log scale values (Dagan, 1989). In this particular case, because the log readings are at regular depth intervals, this becomes straight arithmetic averaging. Figures 7 and 8 show, respectively, the areal and frequency porosity distributions in the Wabiskaw aquifer. The porosity distribution exhibits an areal trend of lower values in the south-southeast, and higher values in the north. Porosity values in the aquifer vary between 14.7% and 32.4%, with an average of 24% (Figure 8). This value is lower than the aquifer average of 31% obtained from core analyses only (Petroleum Geoscience Section, 1993), because, as mentioned previously, the geophysical logs cover the entire aquifer thickness, including shaley streaks not sampled and measured in core analyses. Thus, these porosity distributions and average values are more representative for the Wabiskaw aquifer than the value reported previously.

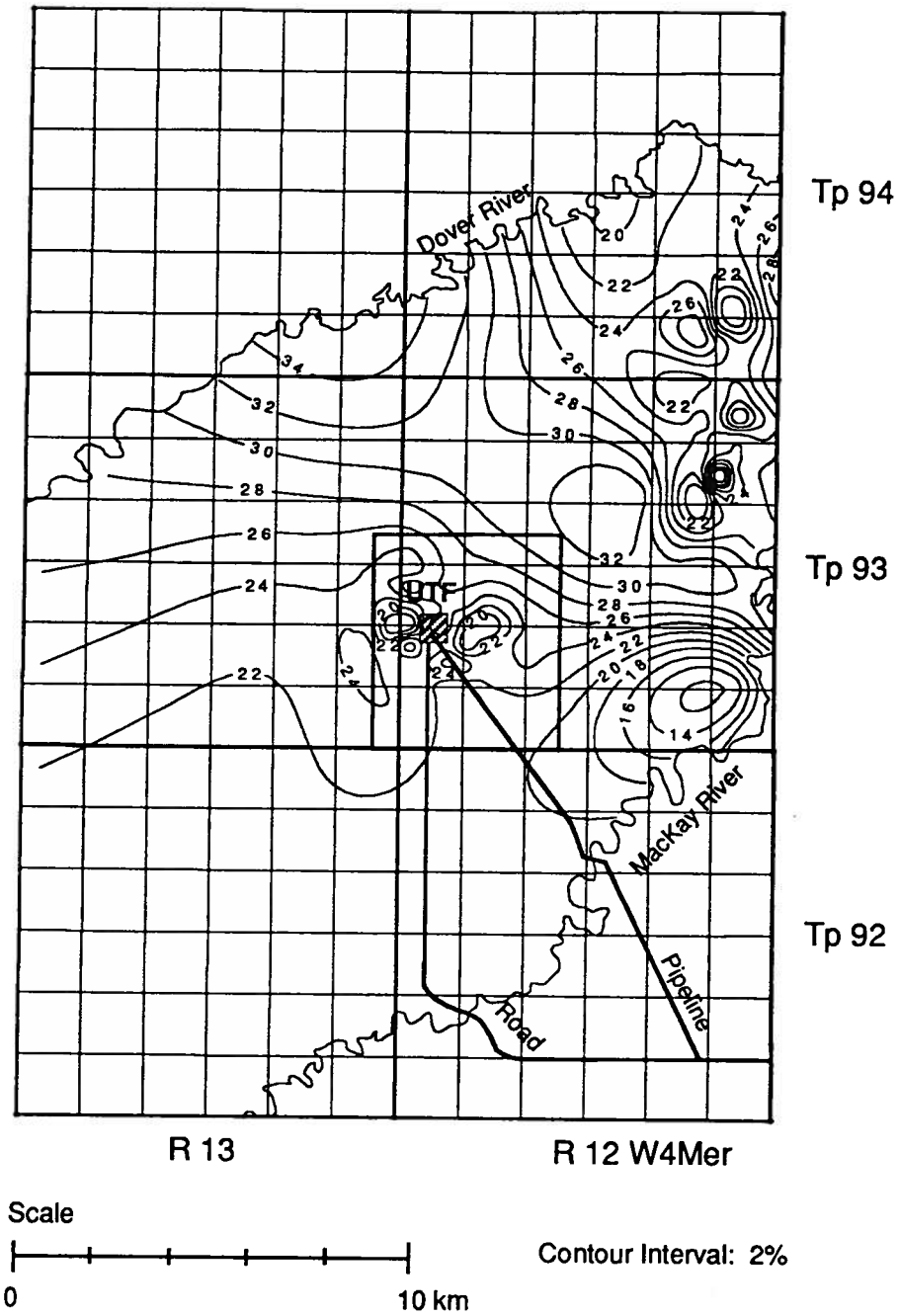


Figure 7: Areal distribution of well-average porosity (%) in the Wabiskaw aquifer.

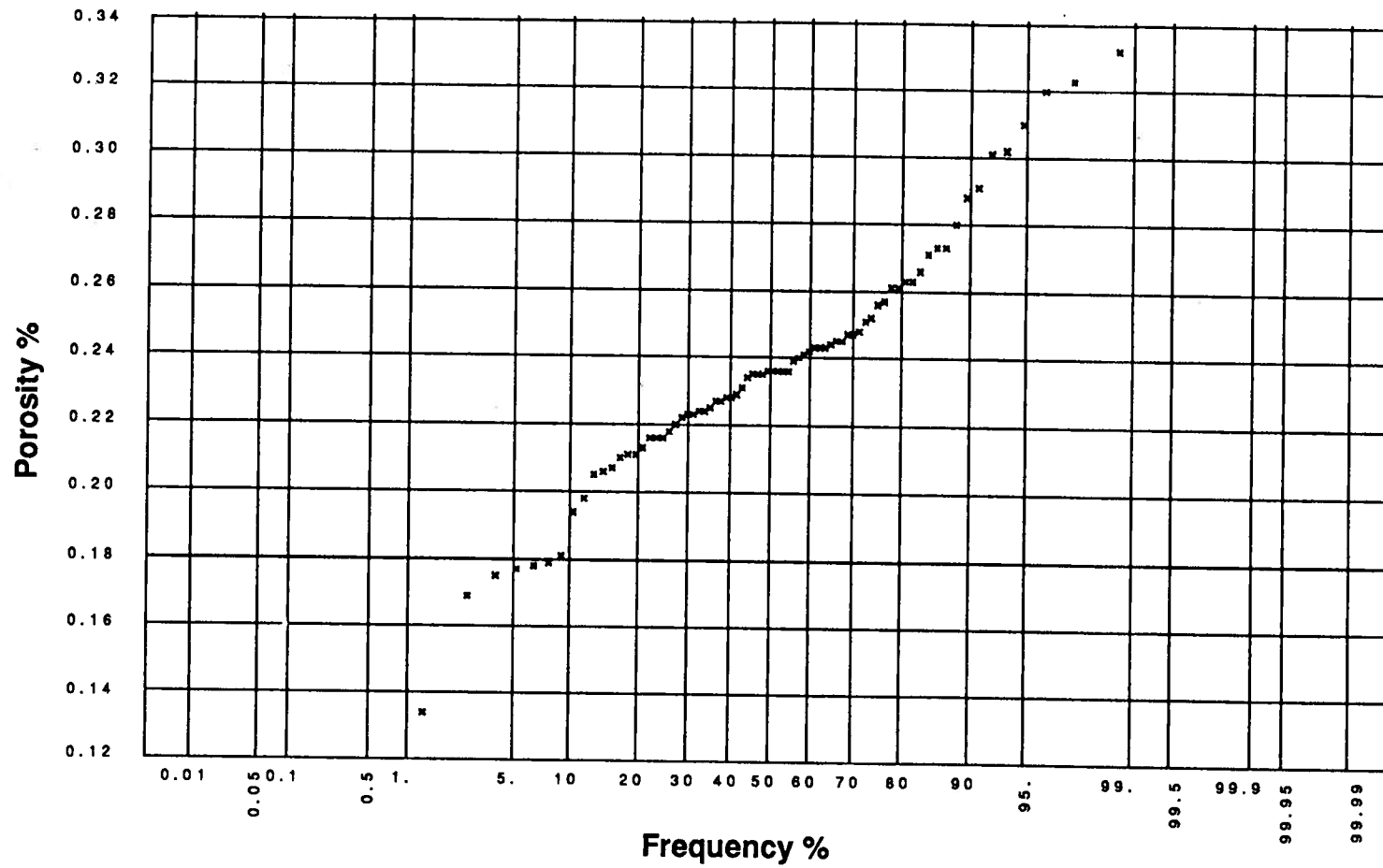


Figure 8: Frequency distribution of well-averaged porosity (%) in the Wabiskaw aquifer.

## Permeability

Unfortunately, very few permeability measurements are available in the local-scale study area for the Wabiskaw aquifer. Seven plug-scale measurements, of which 5 are in the same well, indicate high maximum-permeability values  $k_m$  varying between 2.64 and 6.39 darcies, with a statistical average of 4.11 darcies. No measurements of vertical permeability  $k_v$  were performed, such that there is no direct indication of permeability anisotropy for Wabiskaw sands. However, based on analogy with the McMurray sands for which  $k_m$  and  $k_v$  measurements are available, a vertical anisotropy of  $k_v/k_m = 0.8$  can be assumed for the Wabiskaw sands (Petroleum Geoscience Section, 1993). Besides the plug-scale permeability measurements, four drillstem tests provided information about the well-scale permeability (drillstem tests sample a much larger mass of rock, including less permeable streaks). The drillstem test permeability values for  $k$  vary between 2.9 and 5.7 darcies, with a statistical average of 4.17 darcies. Because of data scarcity, no areal variation of permeability could be ascertained. An attempt was made to correlate permeability with porosity variations, in order to extrapolate the areal porosity distributions into permeability distributions. Unfortunately, no correlation between permeability and porosity was found, either at the plug scale or at the well scale.



## Compressibility and Fracturing Threshold

No new data became available since the previous analysis of these rock properties (Petroleum Geoscience Section, 1993). By comparison with McMurray Formation sands, the bulk compressibility  $c_b$  and pore volume compressibility  $\alpha$  of the Wabiskaw sands are assumed to be  $1.35 \times 10^{-9} \text{ Pa}^{-1}$  and  $0.88 \times 10^{-9} \text{ Pa}^{-1}$ , respectively. These values lead to a specific storage value of  $1 \times 10^{-5} \text{ m}^{-1}$  (Petroleum Geoscience Section, 1993). The specific storage  $S_s$  is defined (de Marsily, 1986) as:

(1)

$$S_s = \rho g [\alpha + \phi (\beta_f - \beta_s)]$$

where  $\rho$  is water density,  $g$  is the gravitational constant,  $\phi$  is porosity,  $\beta_f = 0.47 \times 10^{-9} \text{ Pa}^{-1}$  is water compressibility and  $\beta_s$  is the solid (grain) compressibility of the order of  $10^{-11} \text{ Pa}^{-1}$ . The fracturing threshold of Wabiskaw sands was previously estimated to be 2639 kPa (AOSTRA, 1992).

## EFFECTS OF INJECTION

According to AOSTRA's initial forecast (AOSTRA, 1992), a mixture of produced water, treated blowdown water and regeneration water would be injected into the Wabiskaw aquifer at a rate whose variation is shown in Figure 9. The injection rate is approximated here by a function varying in a stepwise fashion to allow time discretization for numerical modelling purposes. The salinity (total dissolved solids) of the injected water was calculated to be 8,320 mg/l (Petroleum Geoscience Section, 1993), i.e. lower than the salinity of formation water (Figure 5). Previous geochemical modelling (Petroleum Geoscience Section, 1993) has shown that there is no potential for gypsum precipitation or dissolution. The potential for calcite precipitation decreases rapidly with increasing mixing between injected and formation waters, while no dissolution can take place because calcite is absent from the rock matrix. There is potential for dolomite precipitation, but, since the kinetics of dolomite precipitation at low temperatures is slow, no precipitation is expected near the injection well. Similarly, there is potential for quartz precipitation, but this potential decreases with increased mixing with formation water. Moreover, because the low temperature kinetics of  $\text{SiO}_2$  precipitation is very slow, it is expected that quartz precipitation, if any, will take place away from the injection well. It is anticipated that it will take in excess of a hundred years to precipitate half of the silica in solution. Any possible changes in rock properties as a result of water-rock reactions will take place in a much longer time frame than the duration of injection and probably be within the range of data uncertainty caused by measurements error, resolution and

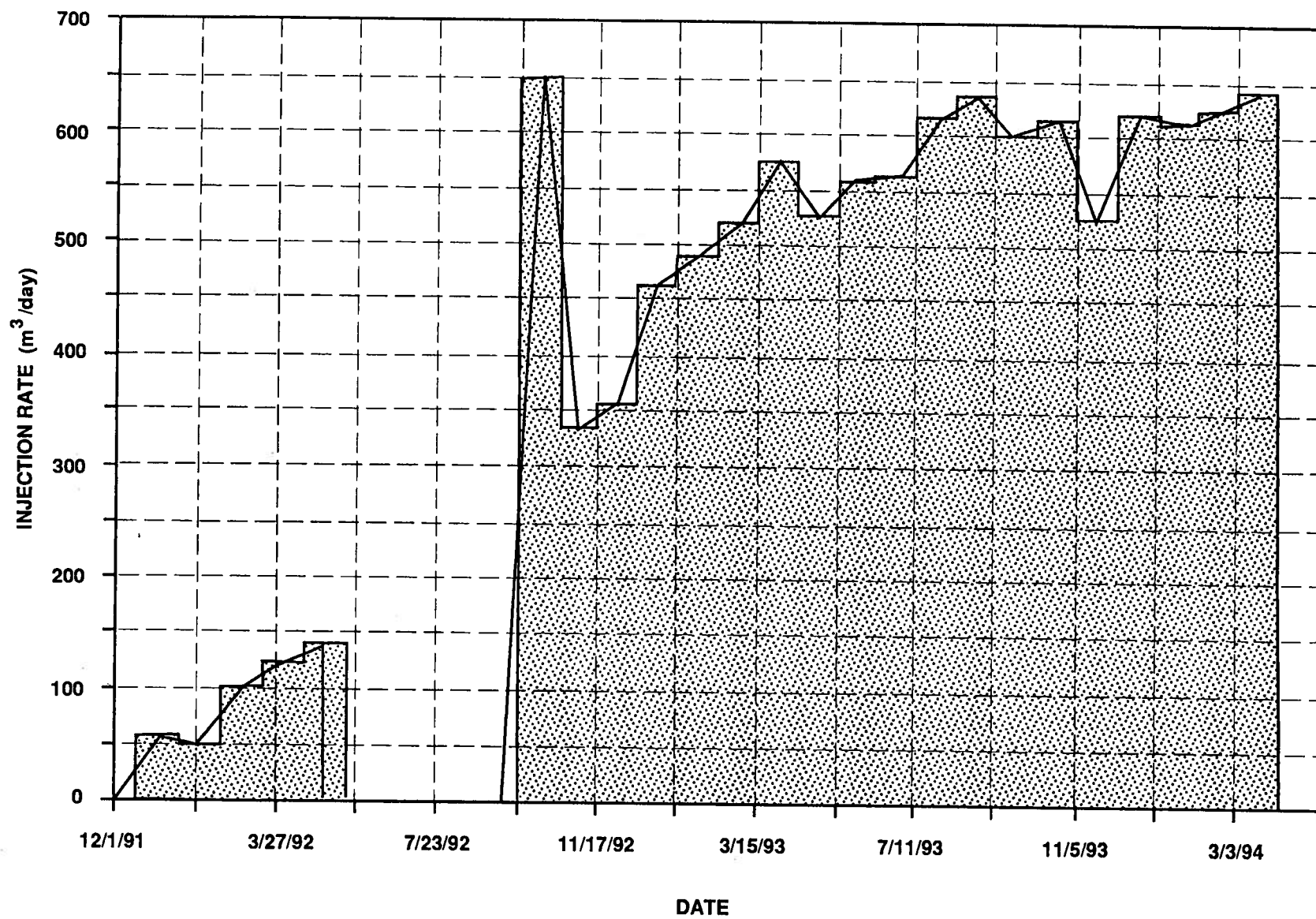


Figure 9: Forecasted injection rate at the UTF site (from AOSTRA, 1992).

distribution. Thus, the geochemical effects of injection may be neglected when examining the hydrodynamic and thermal effects of deep disposal of residual water at the UTF site.

## MATHEMATICAL MODEL

The flow of formation and injected waters in a confined aquifer, including thermal and salinity effects, is described by the equations of momentum and fluid-mass conservation for the fluid, energy conservation for thermal effects, and solute-mass conservation for the dissolved solids. This set of partial differential equations is completed by equations of state describing the variation of fluid properties such as density and viscosity, and by appropriate initial and boundary conditions. The solution of such a complex system of partial differential equations, in a complex geometry, is possible only by numerical means. The mathematical model describing the injection of residual water at the UTF site is presented in the following.

### Fluid Flow

The flow of water in porous media is described by the equation of momentum conservation or Darcy's law (de Marsily, 1986):

(2)

$$\mathbf{v} = - \frac{k}{\mu} (\nabla p + \rho g \nabla z)$$

where  $\mathbf{v}$  is filtration or Darcy velocity,  $k$  is aquifer permeability,  $\mu$  is dynamic viscosity,  $p$  is pressure and  $z$  is the vertical coordinate directed upward. The fluid mass in the aquifer is conserved according to the continuity equation (de Marsily, 1986):

(3)

$$\nabla \cdot (\rho \mathbf{v}) + \frac{\partial}{\partial t}(\phi \rho) + \rho \mathbf{q} = 0$$

where  $\phi$  is aquifer porosity,  $t$  is time and  $\mathbf{q}$  is the volumetric flow rate of injected or pumped water. If the water density and viscosity are constant, then a potential field can be defined using the concept of hydraulic head  $H$  given by:

(4)

$$H = \frac{p}{\rho_o g} + z$$

where  $\rho_o$  is the reference density (usually freshwater) and  $z$  is elevation. By defining the hydraulic conductivity  $K$  as:

(5)

$$K = \frac{\rho g k}{\mu},$$

manipulating Darcy's law (2) and the continuity equation (3), and taking into account the compressibility of the fluid, solid rock and porous matrix (de Marsily, 1986, p. 100-109),

the following "diffusion" equation is obtained for the flow of constant-properties water in a confined aquifer:

(6)

$$\nabla \cdot (K \nabla H) = S_s \frac{\partial H}{\partial t} + q$$

where the specific storage coefficient  $S_s$  was defined previously (relation 1).

Equation (6) was used for a preliminary evaluation of to the hydrodynamic effects of injecting residual water at the UTF site according to the injection rates shown in Figure 9 (Petroleum Geoscience Section, 1993). The basic assumptions underlying the use of equation (6) were that the injected and formation waters had the same (constant) density and viscosity. Also, the Wabiskaw aquifer was considered to have constant porosity ( $\phi = 31\%$ ) and permeability ( $k_m = 4.2$  darcies,  $k_v/k_m = 0.8$ ). Equation (6) was solved numerically using the numerical model Finite Element 3-Dimensional GroundWater (FE3DGW)(Gupta et al., 1984 a,b) based on the finite element discretization shown in Figure 10.

The numerical simulations were carried out with a constant time step  $\Delta t = 10$  days. Figures 11 and 12 show, respectively, the calculated hydraulic head buildup at the node representing the injection well, and the areal spread of the pressure buildup at the end of the injection period (expressed in m of hydraulic head). The hydraulic head buildup of approximately 21 m (Figure 11) was actually obtained not at the injection well itself,

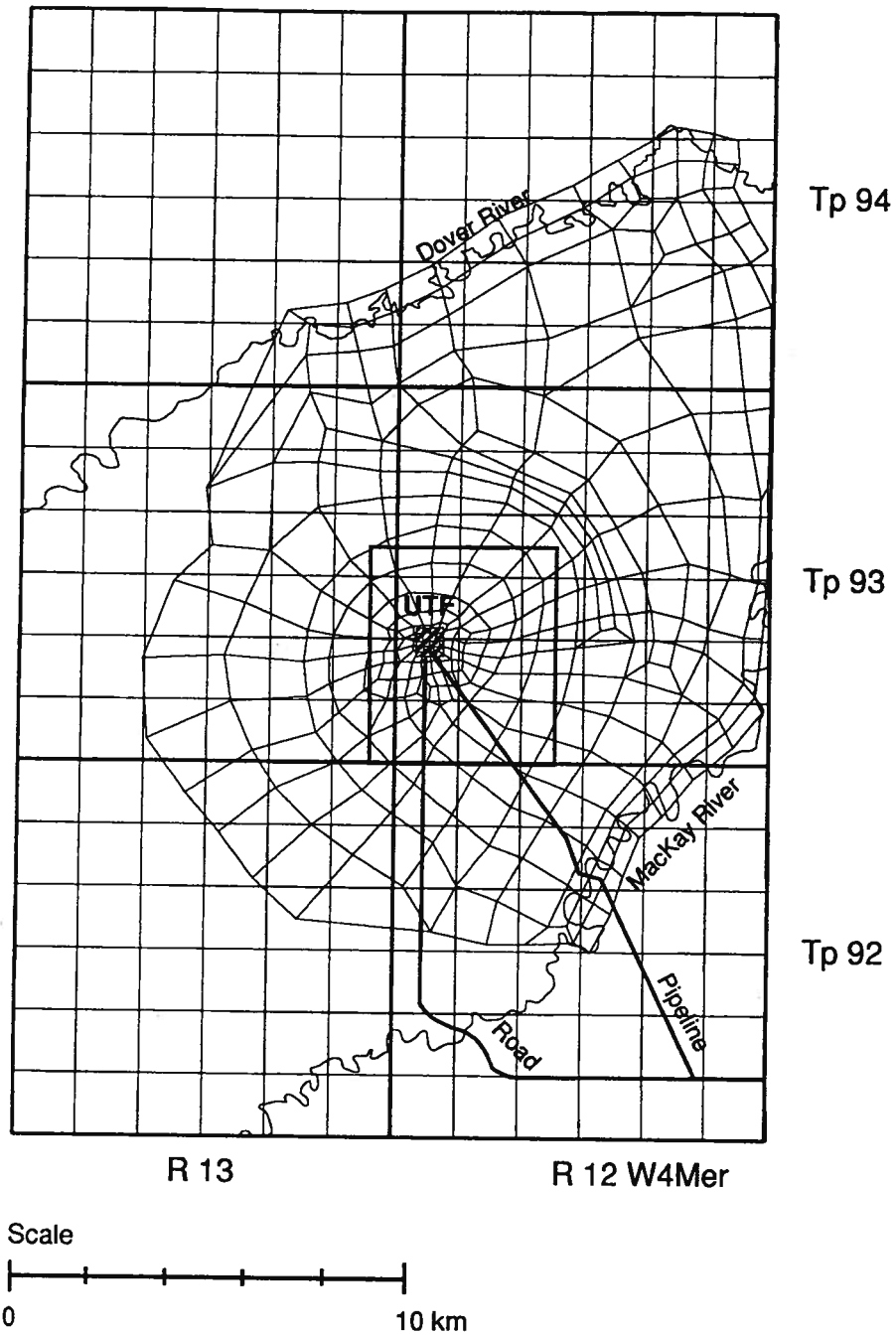


Figure 10: Plan view of the finite element grid used in the numerical simulations of injection.

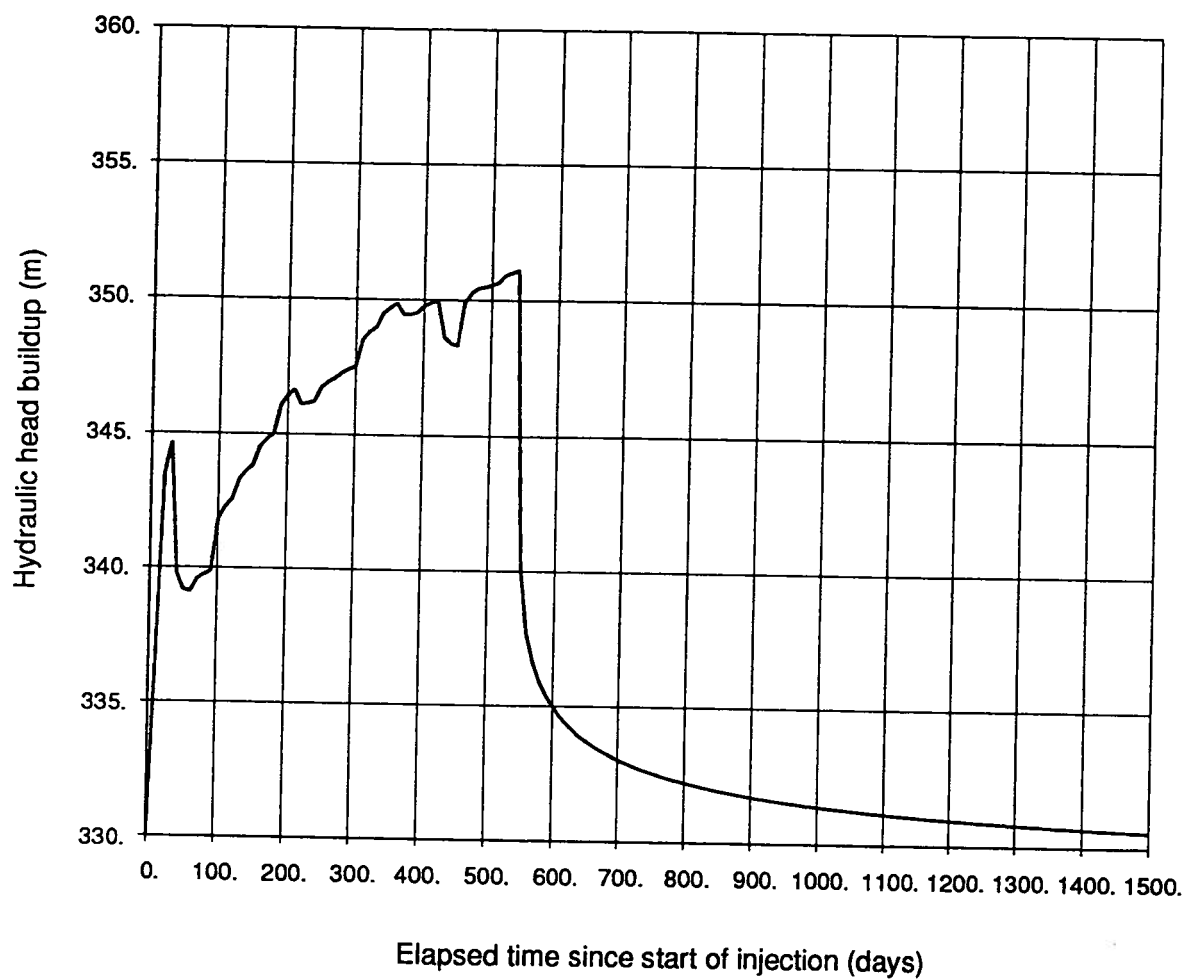


Figure 11: Calculated hydraulic-head buildup at the injection node in the Wabiskaw aquifer, using the FE3DGW numerical model (Petroleum Geoscience Section, 1993).



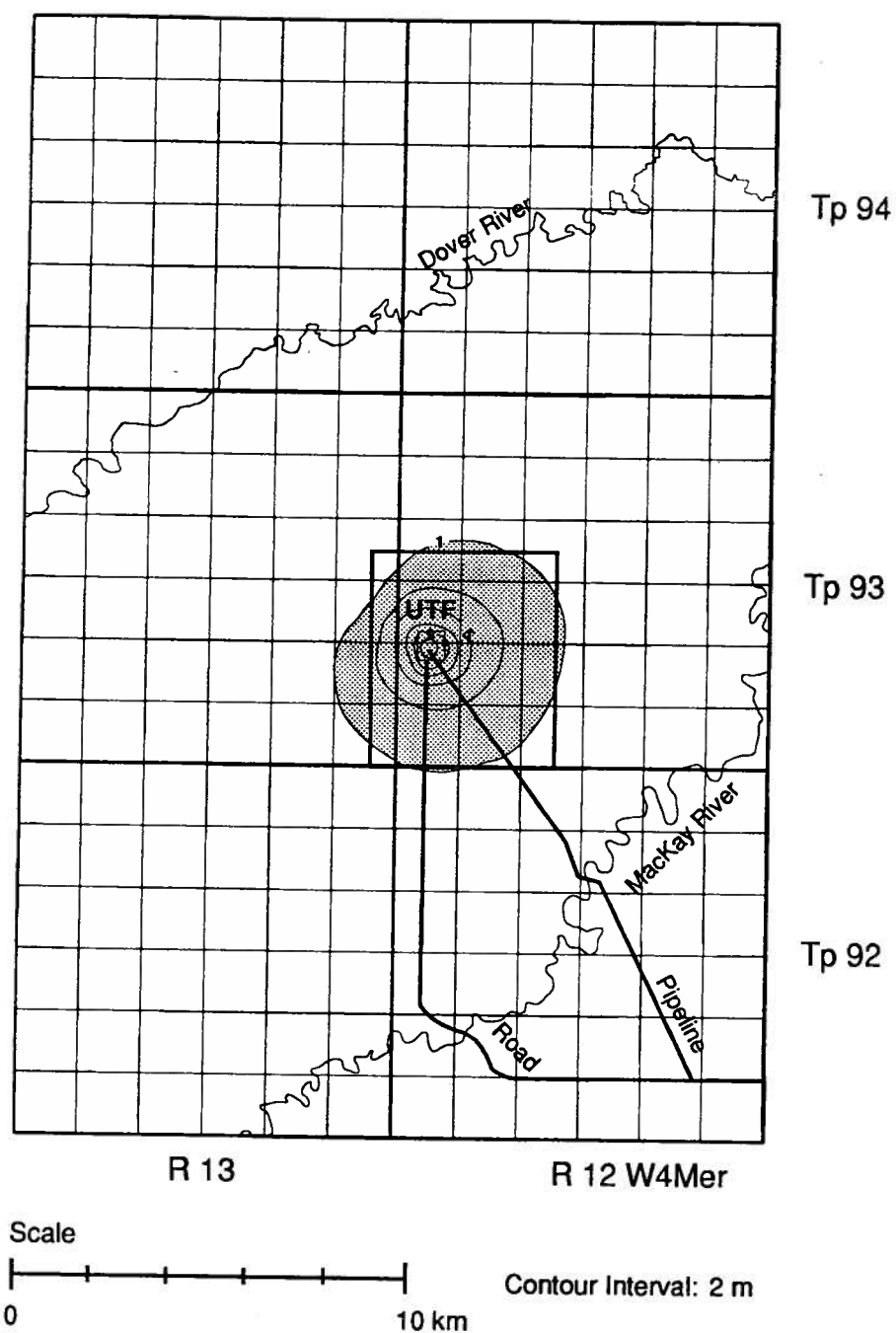


Figure 12: Calculated areal spread of the hydraulic-head (pressure) buildup in the Wabiskaw aquifer at the end of the injection period, using the FE3DGW numerical model (Petroleum Geoscience Section, 1993).

but at an approximate distance (radius of equivalence) of 200 m because of the resolution of the finite element grid used in simulations (Petroleum Geoscience Section, 1993). If, however, neither fluid properties (density and viscosity) nor rock porosity are constant, equation (6) can be used only as a first approximation to simulate the injection of residual water at the UTF site.

The water density is generally a function of pressure, temperature  $T$  and solute concentration  $C$ . By expressing this dependence as a Taylor series and retaining only the first (linear) terms, the following expression is obtained:

(7)

$$\rho(p, T, C) = \rho_o [1 + \beta_f(p - p_o) + c_T(T - T_o) + c_c C]$$

where  $c_T$  is the coefficient of thermal expansion, and  $c_c$  is a coefficient called "composition density ratio" defined (Gupta et al., 1987) as:

(8)

$$c_c = \frac{\rho(C^*, T_o, p_o) - \rho_o}{\rho_o C^*}$$

The subscripts  $f$ ,  $T$ ,  $c$  and  $o$  in relations (7) and (8) refer, respectively, to fluid, temperature, concentration and a reference state, usually freshwater. If the porous rock is compressible, then porosity can be defined as a function of pressure according to:

$$\phi = \phi_o [1 + \alpha(p - p_o)]$$

(9)

After substituting relations (7) and (9) in the continuity equation (3) and rearranging, the following partial differential equation is obtained for the mass conservation of variable-density water in a compressible porous medium:

(10)

$$\nabla \cdot (\rho \mathbf{v}) + \phi \left( \beta_r \frac{\partial p}{\partial t} + c_T \frac{\partial T}{\partial t} + c_c \frac{\partial C}{\partial t} \right) + \rho \phi_o \alpha \frac{\partial p}{\partial t} + \rho q = 0$$

The first term in equation (10) refers to water mass fluxes crossing the surface of a control volume, the second term refers to changes in the fluid mass accumulated inside that volume because of changes in water density resulting from pressure, temperature and salinity variations. The third term refers to changes in the fluid mass accumulated inside the control volume as a result of changes in the pore space caused by pressure variations, and the last term represents sources or sinks corresponding to injection or pumping. Thus, the flow of variable density water is described by the equations of momentum conservation (2) and mass conservation (10).

### Solute Transport

By conserving solute mass in a control volume, the following mass conservation equation is obtained (de Marsily, 1986):

(11)

$$\nabla \cdot (\rho D \nabla C) - \nabla \cdot (\rho v C) - q \rho C' = \frac{\partial}{\partial t} (\rho \phi C)$$

where  $C'$  is the solute concentration of the injected water and  $D$  is the tensor of hydrodynamic dispersion. The first and second terms in equation (11) represent, respectively, dispersive and solute fluxes crossing the surface of the control volume, the third term represents solute mass introduced in the control volume by the injected water, and the last term represents changes in solute concentration inside the control volume. The hydrodynamic dispersion tensor  $D$  has three components, one longitudinal along the velocity vector:

(12)

$$D_L = \epsilon_L |v| + D_m^*$$

and two transverse components, normal to the velocity vector and at 90° one from another:

(13)

$$D_T = \epsilon_T |v| + D_m^*$$

In relations (12) and (13),  $\epsilon$  represents the solute dispersivity (length dimensions) and the subscripts L and T stand for longitudinal and transverse, respectively. The coefficient of molecular diffusion in porous media  $D_m^*$  depends on the medium type. For sand and sandstones,  $D_m^*$  can be approximated by the empirical relation:

$$D_m^* = \phi D_m$$

Where  $D_m$  is the coefficient of molecular diffusion in water. The mechanical dispersion expressed by the term  $\epsilon|v|$  in relations (12) and (13) is due to the tortuous flow path through the pore space (Bear, 1972). Thus, equation (11) and relations (12) - (14) describe the mass conservation of a non-reactive substance dissolved in the injected and formation waters.

### Heat Transfer

Unlike a dissolved substance (solute), heat is transferred in a porous medium not only by the moving fluid (in this instance water) but also by the solid rock matrix. In a porous medium saturated with a flowing fluid, heat at low temperatures is transported by three main mechanisms: (1) conduction through the solid and fluid; (2) convection or advection by the moving fluid; and (3) dispersion caused by the tortuosity of the pore space, in a process similar to solute dispersion. The transport of heat is governed by the law of energy conservation, which, for constant specific heat  $c$ , can be written with temperature as the dependent variable as follows:

$$\nabla \cdot (\lambda \nabla T) - \nabla \cdot (\phi \rho_f c_f v T) - q \rho_f c_f T' = \frac{\partial}{\partial t} [(\rho c)_m T]$$

where  $\lambda$  is the tensor of equivalent conductivity,  $(\rho c)_m$  is the heat capacity of the water saturated porous medium, and  $T'$  is the temperature of the injected or pumped water. The first term in equation (15) represents heat fluxes crossing the surface of a control volume by thermal conduction and dispersion, the second term represents heat carried by the flowing water, the third term represents heat introduced into or taken from the control volume by the injected or pumped water, and the last term represents heat accumulated inside the control volume. The heat capacity of the saturated porous medium is given by the porosity-weighted arithmetic average of the water and rock heat capacities, according to the relation:

(16)

$$(\rho c)_m = \phi \rho_f c_f + (1 - \phi) \rho_s c_s$$

where the subscripts m, f and s refer to the porous medium, fluid and solid, respectively. By analogy with the dispersion tensor for a solute (relations 12 and 13), the longitudinal and transverse components of the tensor of equivalent conductivity  $\lambda$  can be written as (de Marsily, 1986):

(17)

$$\lambda_L = \lambda_m + \rho_f c_f \epsilon_L^T |v|$$

$$\lambda_T = \lambda_m + \rho_f c_f \epsilon_T^T |v|$$

where  $\lambda_m$  is the thermal conductivity of the water saturated porous medium, and  $\epsilon_L^T$  and  $\epsilon_T^T$  are thermal dispersivities (also length dimensions). Finally, the thermal conductivity  $\lambda_m$  is usually expressed as the porosity-weighted geometric average of the water (fluid) and rock (solid) thermal conductivities (Bachu, 1991), according to the relation:

(19)

$$\lambda_m = \lambda_s^{1-\phi} \lambda_f^\phi$$

Thus, the partial differential equation (15) together with relations (16 - 19) describe the transfer of heat in saturated porous media.

### Initial and Boundary Conditions

In order to solve the system of partial differential equations describing fluid flow, mass (solute) transport and heat transfer as a result of injection of residual water at the UTF site, there is need to define the initial (prior to injection) and boundary conditions of the system. For fluid flow, the natural (baseline) distribution of hydraulic heads in the Wabiskaw aquifer (Figure 6) is considered as the initial condition. As boundary conditions for fluid flow, the hydraulic heads around the edge of the finite element grid (Figure 10)

were maintained constant, based on the results of previous simulations (Petroleum Geoscience Section, 1993) which have shown that the pressure buildup will not reach the edges of the model area. For solute transport, the natural salinity distribution in Wabiskaw formation water (Figure 5) was considered for initial conditions. Because the Wabiskaw aquifer is confined, there is no solute transport across the top and bottom aquifer boundaries, a condition expressed by:

(20)

$$\frac{\partial C}{\partial t} = 0$$

For heat transfer, an initial temperature of 7°C was considered for the Wabiskaw aquifer, based on its depth and geothermal gradients (approximately 25°C/km) (Bachu and Burwash, 1991). Although there is no fluid flow through the confining aquitards, heat escapes through the top and bottom boundaries of the Wabiskaw aquifer through conduction. Thus, heat transfer in these aquitards takes place according to the conduction equation:

(21)

$$\nabla \cdot (\lambda \nabla T) = \frac{\partial}{\partial t} [(\rho c)_m T]$$

Heat fluxes across the aquifer-aquitard boundaries must be equal resulting in the boundary condition:



$$\lambda_m \frac{\partial T}{\partial z} \big|_{aqt} = \lambda_m \frac{\partial T}{\partial z} \big|_{aqf}$$

where the subscripts aqt and aqf stand for aquitard and aquifer, respectively.

Thus, the mathematical model for simulating hydrodynamic, hydrochemical and thermal effects of injection of residual water at the UTF site consists of the system of partial differential equations (2), (10), (11), (15) and (21) for the conservation of momentum, fluid mass, solute mass and energy, constitutive relations (7) - (9), (12) - (14), and (16) - (19), and appropriate initial and boundary conditions. This system of partial differential equations is coupled and non-linear. The fluid velocity distribution affects the temperature and solute distributions through the advective and dispersive terms. The temperature and concentration distributions affect in turn the flow through their effect on water properties (density and viscosity). The solution of this system of partial differential equations is possible only by using numerical methods.

The finite element model CFEST (Coupled Fluid, Energy and Solute Transport) developed by Battelle Memorial Institute (Gupta et al., 1987) was used for the numerical simulation of injection of residual water at the UTF site. A series of assumptions and approximations are inherently made in mathematical modelling and computer simulations, which must be taken into account when assessing the results. The basic assumptions

used in the development of the mathematical model on which CFEST is based (Gupta et al., 1987) are:

1. fluid flow is Darcian and transient;
2. permeability tensor main axes are collinear with the axes of coordinates;
3. fluid density is a function of pressure, temperature and solute concentration according to relation (7);
4. fluid viscosity is a function of temperature and concentration;
5. the injected fluid is miscible with the resident aquifer fluids;
6. aquifer properties (porosity, permeability, thickness) vary spatially (the thickness variations are nodal, while material properties are element-constant);
7. hydrodynamic dispersion is a function of fluid velocity according to relations (12) (13), (17) and (18);
8. boundary conditions permit natural water movement in the aquifer and heat losses or gains to adjacent formations;
9. the porous media and water are compressible;
10. the porous media and water are in thermal equilibrium;
11. rock density and specific heat remain constant; and
12. viscous dissipation is negligible with respect to energy balance.

In numerical modelling there are approximations and round-off errors inherent in the numerical method and space and time discretization. Because of grid resolution, the values obtained at any node, including the one representing the injection site, are not the

actual values at the injection well. They represent values to be found at an equivalent distance (radius)  $r_e$  from the well which depends on the type and scale of the model, grid resolution and system characteristics. For the finite element grid used in the present simulations (Figure 10), it is estimated that the radius of equivalence for the injection node is approximately  $r_e = 200\text{m}$  (Petroleum Geoscience Section, 1993).

For calibration purposes, the natural (baseline) potentiometric surface of the Wabiskaw aquifer (Figure 6) was calculated using the CFEST model without considering any thermal or salinity effects. For steady-state fluid flow in an aquifer, the diffusion equation (6) simply becomes:

(23)

$$\nabla \cdot (K \nabla H) = 0$$

Figure (13) shows the computed steady-state potentiometric surface of the Wabiskaw aquifer in the area of interest. Comparison of Figures (6) and (13) indicates a good match between observed and calculated hydraulic head distributions. Differences, where they exist, are most probably caused by inaccuracies and coarse resolution in obtaining the observed hydraulic head distribution (Petroleum Geology and Basin Analysis Group, 1992). The mathematical and numerical models inherently conserve fluid mass, adjusting the potentiometric surface accordingly, which may not necessarily be the case for the observed hydraulic-head distribution obtained from sparse data. The calculated potentiometric surface (Figure 13) was considered as initial condition for fluid flow in the Wabiskaw aquifer in all subsequent simulations.

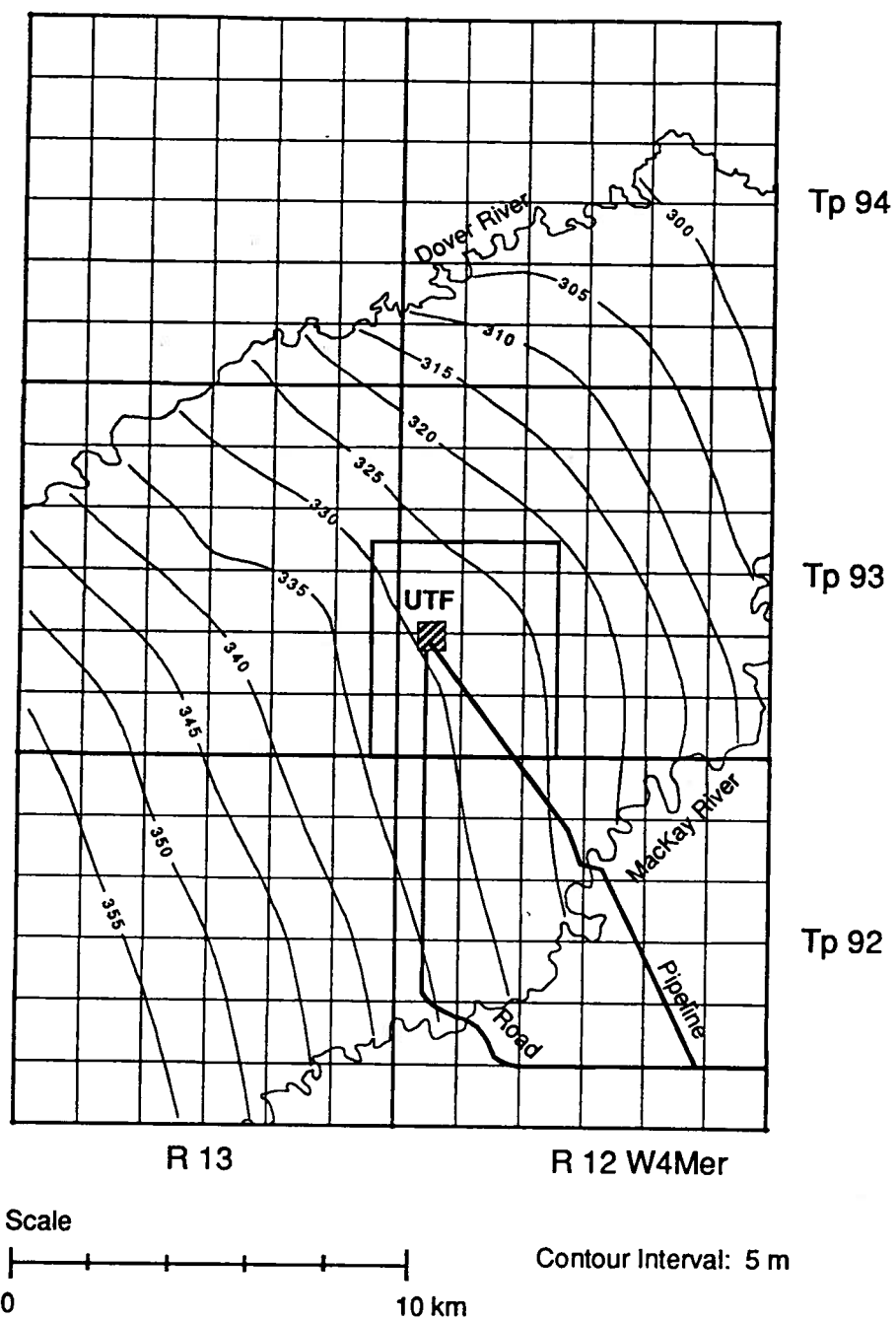


Figure 13: Calculated (simulated) distribution of baseline freshwater hydraulic-head (m) in the Wabiskaw aquifer, using the CFEST numerical model (Gupta et al., 1987).

## **SIMULATION OF INJECTION**

The injection of residual water at the UTF site was simulated for the period August, 1992 - March, 1994 using the injection rate  $q$  forecasted by AOSTRA (AOSTRA, 1992). The simulated injection period is actually less than two years because the initial rates of injection are low and are followed by a four-month pause in injection (Figure 9), during which any hydraulic-head buildup and other effects would probably dissipate away. The injection rate was approximately by a stepwise function with a time step of  $\Delta t = 10$  days (Figure 9) in order to optimize computer resources. Previous simulations with the model FE3DGW have shown that this time step is appropriate for simulations (Petroleum Geoscience Section, 1993). The temperature and salinity of the injected water were maintained constant at 80°C and 8300 mg/l, respectively. The simulations were carried out in two stages. In the first stage, only hydrodynamic effects were considered by simulating the injection of residual water assumed to have the same temperature and salinity as the aquifer water. This simulation allowed a comparison between the results obtained with the FE3DGW and CFEST models, and also an evaluation of the effects of considering a variable porosity distribution in the Wabiskaw aquifer. In the second stage, thermal and salinity effects were evaluated by considering the injected water as having different properties than the aquifer water.

## Hydrodynamic Effects

Simulation of fluid flow only amounts to solving equation (10) in which the water density is assumed to be constant ( $\beta_t = c_T = c_c \equiv 0$ ) and only the porosity  $\phi$  varies as a function of pressure according to relation (9). Figures 14 and 15 show the simulated pressure buildup at the injection node and the areal spread of the pressure buildup, respectively, both expressed in m of equivalent hydraulic head (relation 4). The variation in hydraulic head buildup (Figure 14) closely follows the variation in the injection rate (Figure 9). After the cessation of injection, the hydraulic head (pressure) buildup will rapidly decay to pre-injection conditions (Figure 14) because of the high aquifer hydraulic diffusivity. The calculated hydraulic-head buildup at the end of the period is  $\Delta H = 55.5$  m (Figure 14), compared with the buildup of  $\Delta H = 52$  m obtained previously with the FE3DGW numerical model (Figure 11). The difference is due mainly to the fact that the porosity of the Wabiskaw aquifer at the UTF site is around 22 - 24% (Figure 7), lower than the value of 31% used in the previous simulations with the FE3DGW numerical model (Petroleum Geoscience Section, 1993). Another possible reason, thought of being of secondary importance in this case, is the fact that the CFEST numerical model allows for porosity variations with pressure (relation 9), while the FE3DGW model considers porosity as being constant. As the pressure increases with injection, porosity decreases as a result of compression, with the result that less pore volume is available for the accumulation of injected water, leading in turn to higher incremental pressure. However, because the whole range of pressure increase is relatively small, this effect is less

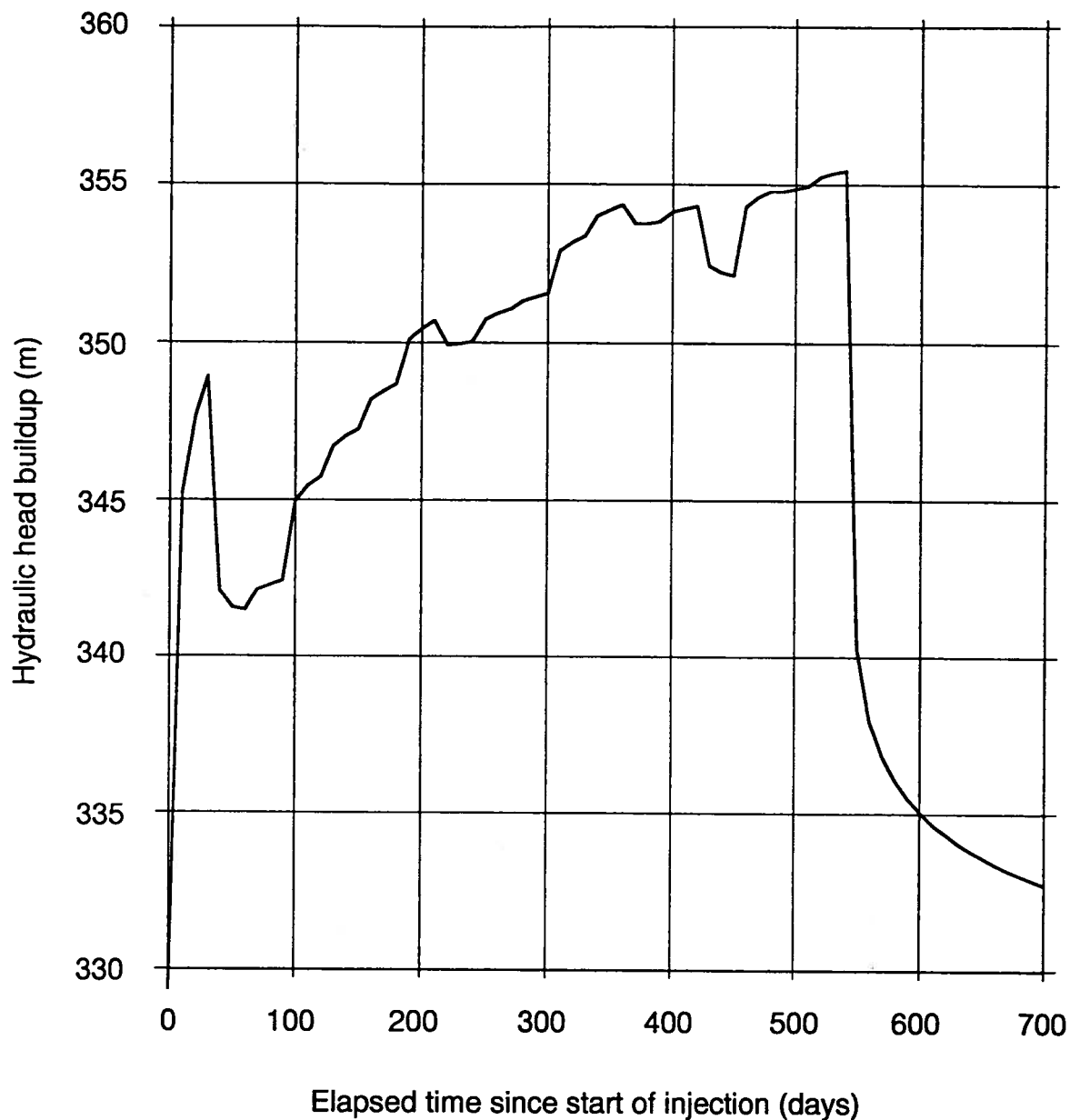


Figure 14: Calculated hydraulic-head buildup at the injection node in the Wabiskaw aquifer, using the CFEST numerical model and assuming the same properties for injected and aquifer waters.

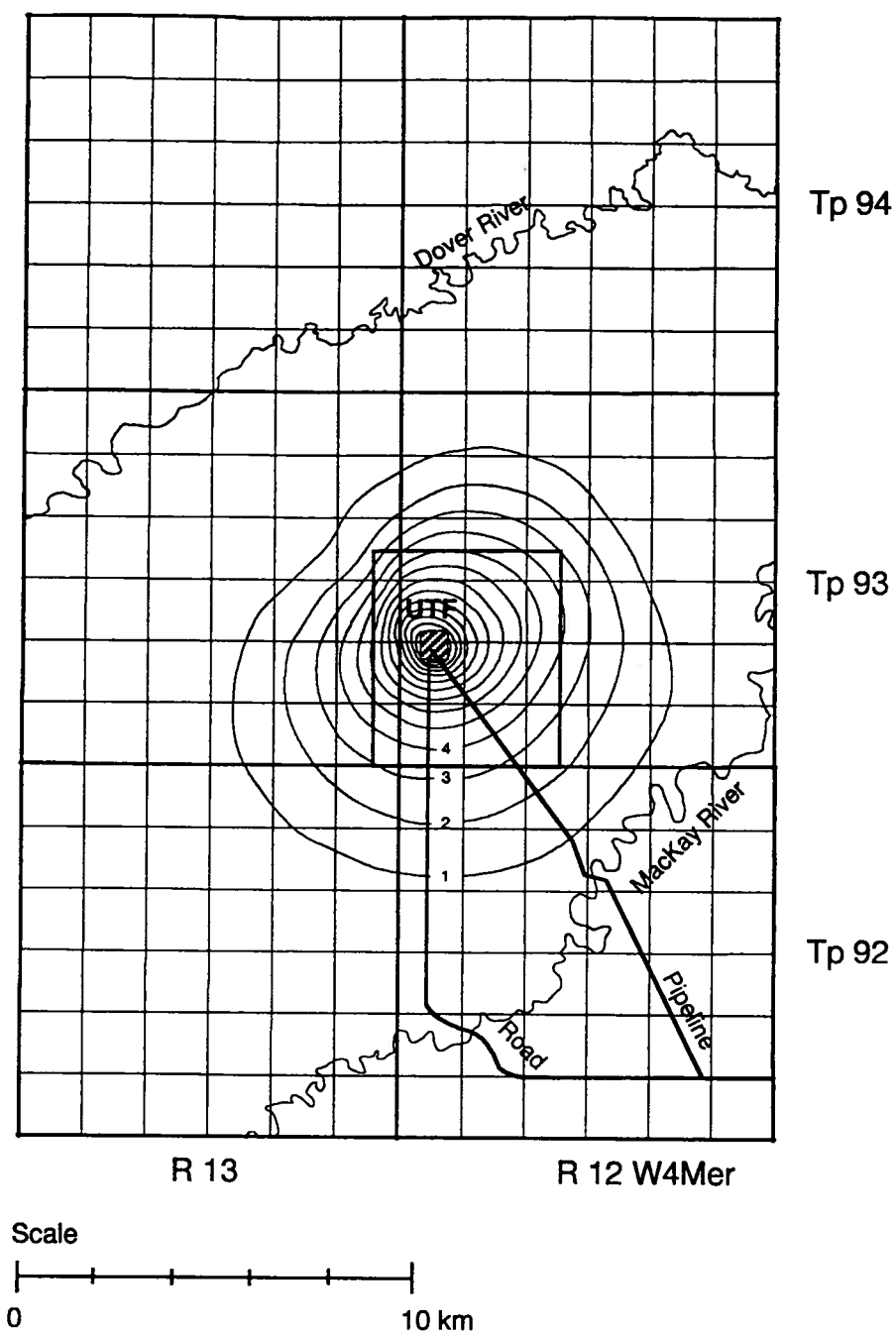


Figure 15: Calculated areal spread of hydraulic-head buildup in the Wabiskaw aquifer at the end of the injection period, using the CFEST numerical model and assuming the same properties for injected and aquifer waters.



important in this case than the fact that the porosity value used in the current simulations is lower than in the previous ones. Because of the resolution of the finite element grid, the hydraulic-head buildup at the injection node represents in reality the hydraulic-head buildup at an approximate distance of 200 m from the injection well. The hydraulic head equivalent to 90% of the fracturing pressure is 550.7 m, corresponding to a buildup of 220.7 m. Although the calculated buildup of 56 m at the injection node is at some distance from the injection well itself, it is believed that the pressure in the aquifer will remain at all times below 90% of the fracturing pressure. It is possible to estimate the hydraulic head (pressure) buildup at the injection well by using analytical methods. However, application of any analytical method requires a set of simplifying assumptions and the numerical solution of a convolution integral (de Marsily, 1986). For example, if one assumes the aquifer as being isotropic, homogeneous and of constant thickness and infinite lateral extent, the hydraulic head buildup in the case of constant-rate injection through a fully-penetrating well is given by an exponential integral (Theis' solution). For a variable rate of injection, the solution of the flow equation (6) becomes a convolution integral (de Marsily, 1986) which requires also a numerical solution. Such a solution was not attempted here because of the inherent simplifying assumptions and the need for complex numerical integration.

The areal spread of pressure buildup in the Wabiskaw aquifer at the end of the injection period, as indicated by the contour of the hydraulic-head increase  $\Delta H = 1$  m is asymmetric (Figure 15), reaching between 4 km in the northwest and 6 km in the southeast. The areal spread obtained in the previous simulation with the FE3DGW model is smaller (Figure 12). The difference is again attributed to lower porosity considered in

the current simulations. The asymmetry of the cone of pressure buildup (Figure 15) is most probably caused by lower porosity in the southeast than in the northwest (Figure 7). Generally, the current simulations of injection performed considering a more realistic porosity distribution in the Wabiskaw aquifer indicate a larger pressure buildup, but still within the safety limits imposed by regulatory agencies.

### Thermal and Salinity Effects

The second set of simulations was carried out taking into account the different temperature and salinity of the injected water from the aquifer water. This amounts to solving the simultaneous, coupled system of partial differential equations (10), (11) and (15) together with the constitutive relations (7), (8), (12) - (14) and (16) - (19). The following values were considered for the various parameters involved in these equations and relations:

- coefficient of water thermal expansion  $c_T = 2 \times 10^{-4} \text{ } ^\circ\text{C}^{-1}$  (de Marsily, 1986);
- longitudinal solute dispersivity  $\epsilon_L = 50 \text{ m}$  (Domenico and Schwartz, 1990);
- transverse solute dispersivity  $\epsilon_T = 0.1 \epsilon_L$  (Domenico and Schwartz, 1990);
- coefficient of molecular diffusion  $D_m = 3 \times 10^{-7} \text{ m}^2/\text{s}$  (Li and Gregory, 1974);
- water specific heat  $c_f = 4185 \text{ J/m}^3 \text{ } ^\circ\text{C}$  (de Marsily, 1986);
- rock specific heat  $C_s = 960 \text{ J/m}^3 \text{ } ^\circ\text{C}$
- water thermal conductivity  $\lambda_f = 0.63 \text{ W/m } ^\circ\text{C}$  (de Marsily, 1986);
- rock thermal conductivity  $\lambda_s = 3 \text{ W/m } ^\circ\text{C}$  (Bachu, 1993);

Figures 16 and 17 show the calculated pressure buildup at the injection node and the areal spread of pressure buildup at the end of the injection period, respectively, expressed in m of hydraulic head. Comparison of Figures 14 and 16 shows only a marginal effect of higher temperature and lower salinity of the injected water. The pressure is higher at the injection node by the equivalent of 0.5 m hydraulic head (5 kPa) because of water thermal expansion (the volume of water is slightly higher at higher temperatures). This effect, nevertheless, is negligible.

Figure 18 shows the calculated temperature increase at the injection node. Again, it must be noted that the injection node is equivalent to a distance of approximately 200 m from the injection well. For this reason, the calculated temperature reaches only 22°C, although the temperature of the injected water is considered to be 80°C. Heat is transferred by conduction from the injected water to the formation water and rock. Also, heat is lost through the upper and lower aquifer boundaries. Because of heat transfer and heat losses, the temperature of the injected water decreases relatively rapidly, such that, unlike the pressure buildup, the temperature in the aquifer increases above the baseline initial value only for a relatively short distance from the injection well (approximately 300 - 400 m). After the cessation of injection, the temperature will decrease very slowly (Figure 18) because the heat accumulated in the rock and fluid mass will dissipate only by conduction to the surrounding aquifer and overlying and underlying aquitards.

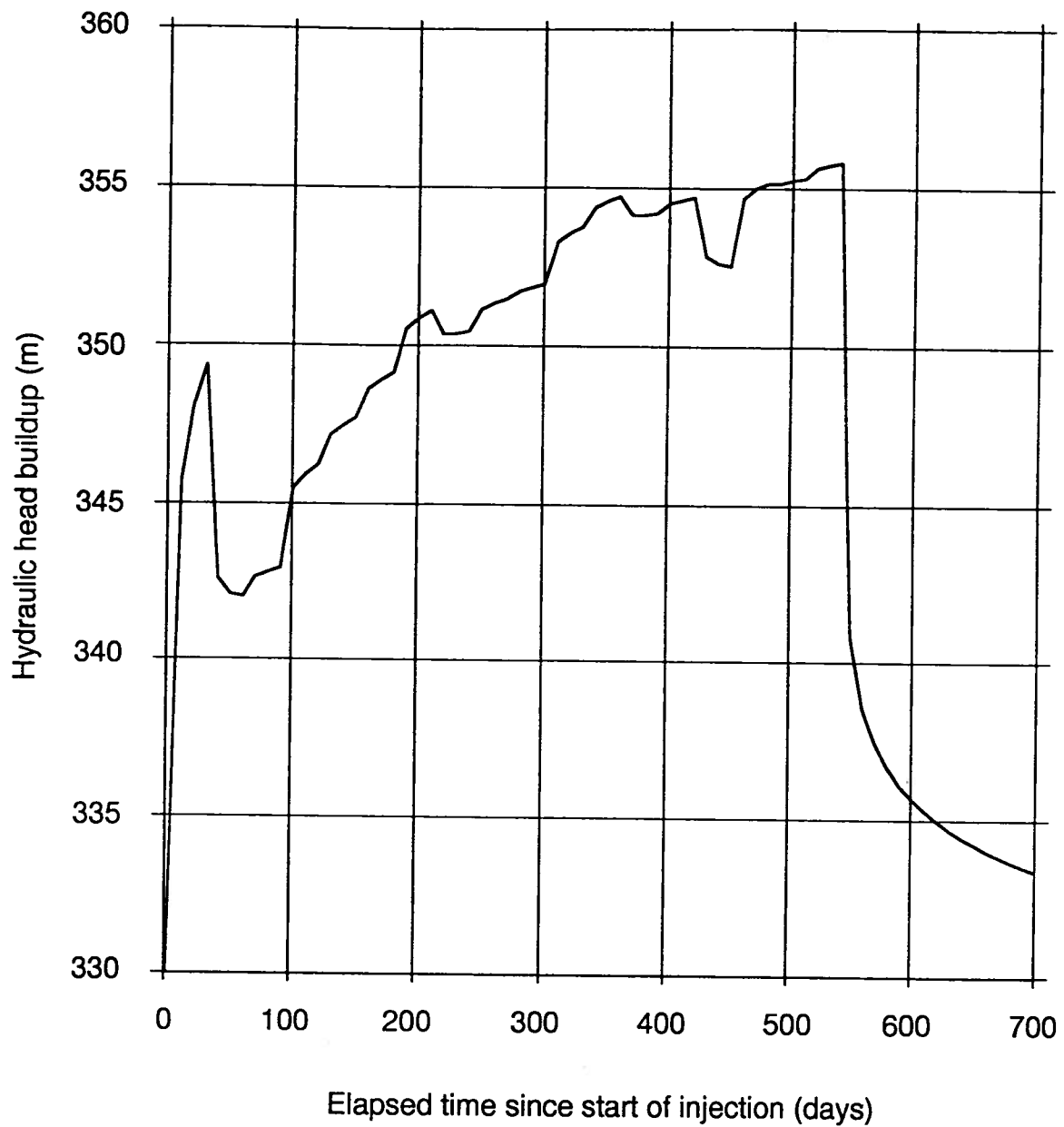


Figure 16: Calculated hydraulic-head buildup at the injection node in the Wabiskaw aquifer, using the CFEST numerical model, for properties of injected water different from those of the aquifer water.

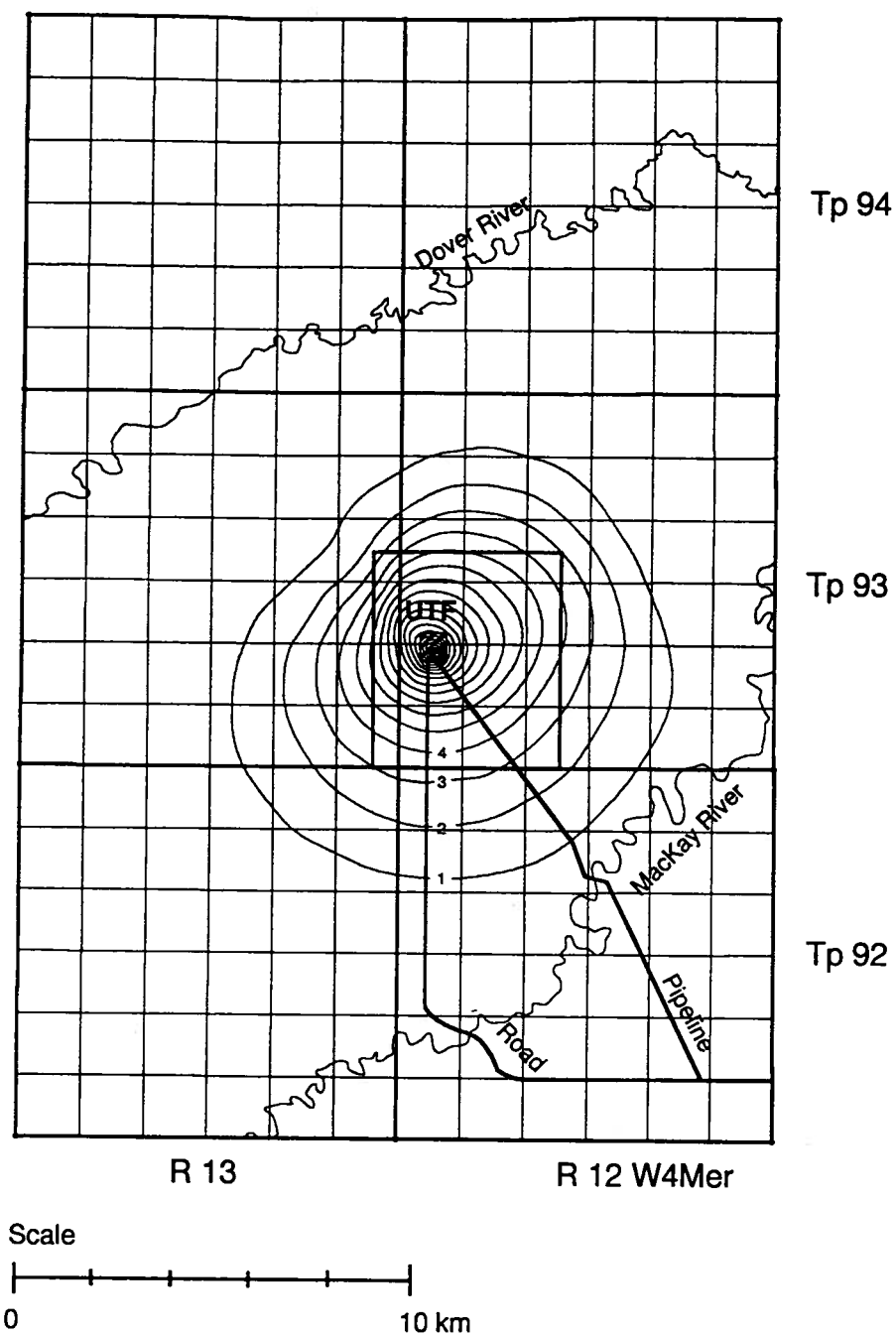


Figure 17: Calculated areal spread of hydraulic-head buildup in the Wabiskaw aquifer at the end of the injection period, using the CFEST numerical model, for properties of injected water different from those of the aquifer water.

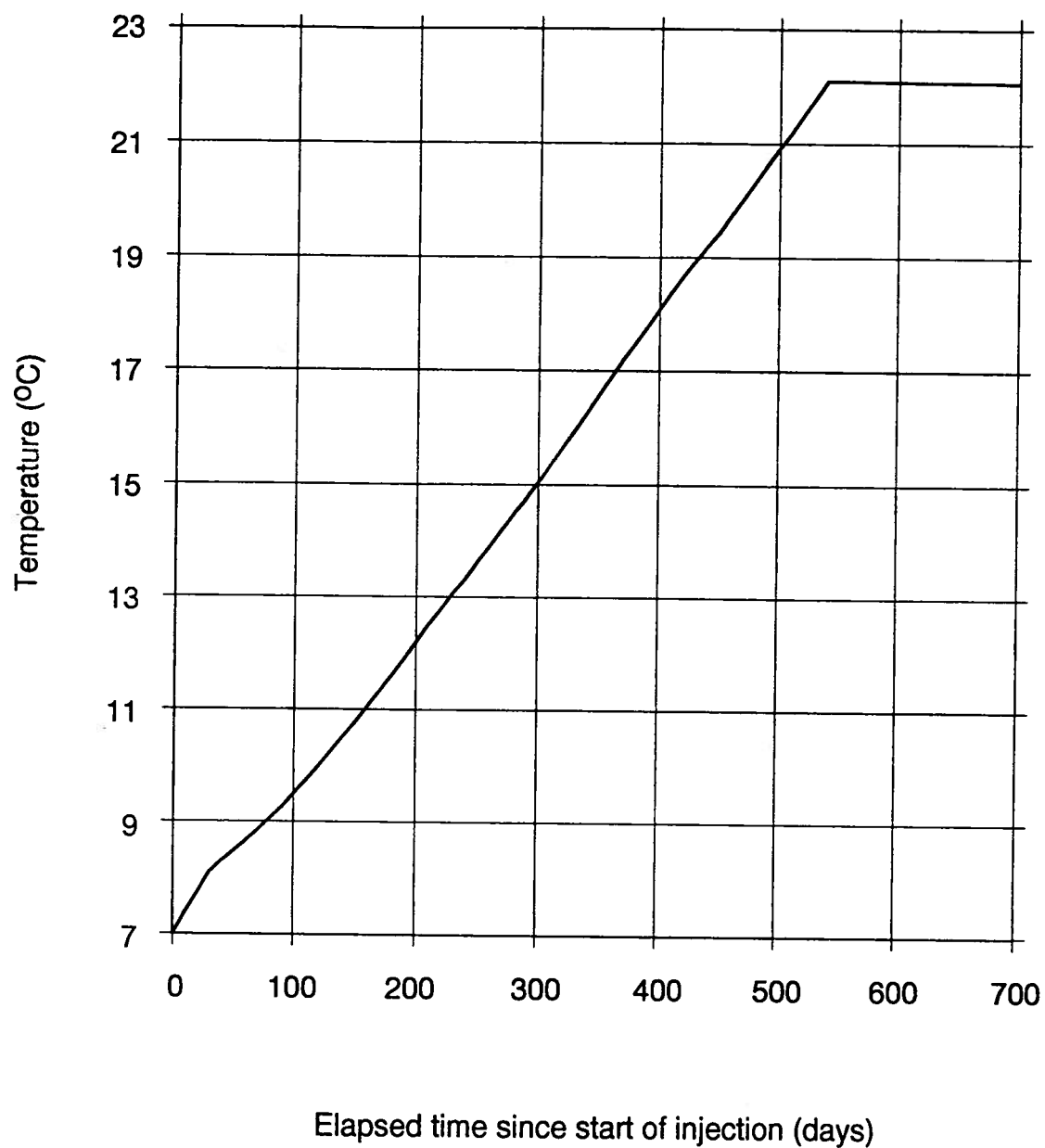


Figure 18: Calculated temperature increase at the injection node in the Wabiskaw aquifer.

Figure 19 shows the variation in water salinity at the injection node. Because the salinity of the injected water is lower than that of the aquifer water (8,300 mg/l versus 12,000 mg/l), the water salinity at the injection node will actually decrease through mixing between the two. As a result, a dilution plume will form, whose spread at the end of the injection period is shown in Figure 20. The spread of the dilution plume is slightly asymmetric, reaching approximately 500 m northeast from the injection site, but only approximately 300 - 350 m in other directions. The difference is attributed to the effect of the northeastward flow of formation waters (Figure 6), which is superimposed over the hydrodynamic effects of injection. After the cessation of injection, the pressure buildup will decrease rapidly (Figure 16) and the initial pressure regime in the aquifer will be re-established. As a result, the dilution plume formed during injection will be subjected to hydrodynamic advection and dispersion caused by the natural hydraulic gradient of formation waters of approximately 2 m/km (Figure 6). For an assumed aquifer permeability of  $4 \times 10^{-12} \text{m}^2$  (4 darcies), this corresponds to a Darcy velocity of approximately 2.5 m/a. At this velocity, it will take well over 1000 years for the dilution plume to reach discharge areas along the MacKay River.

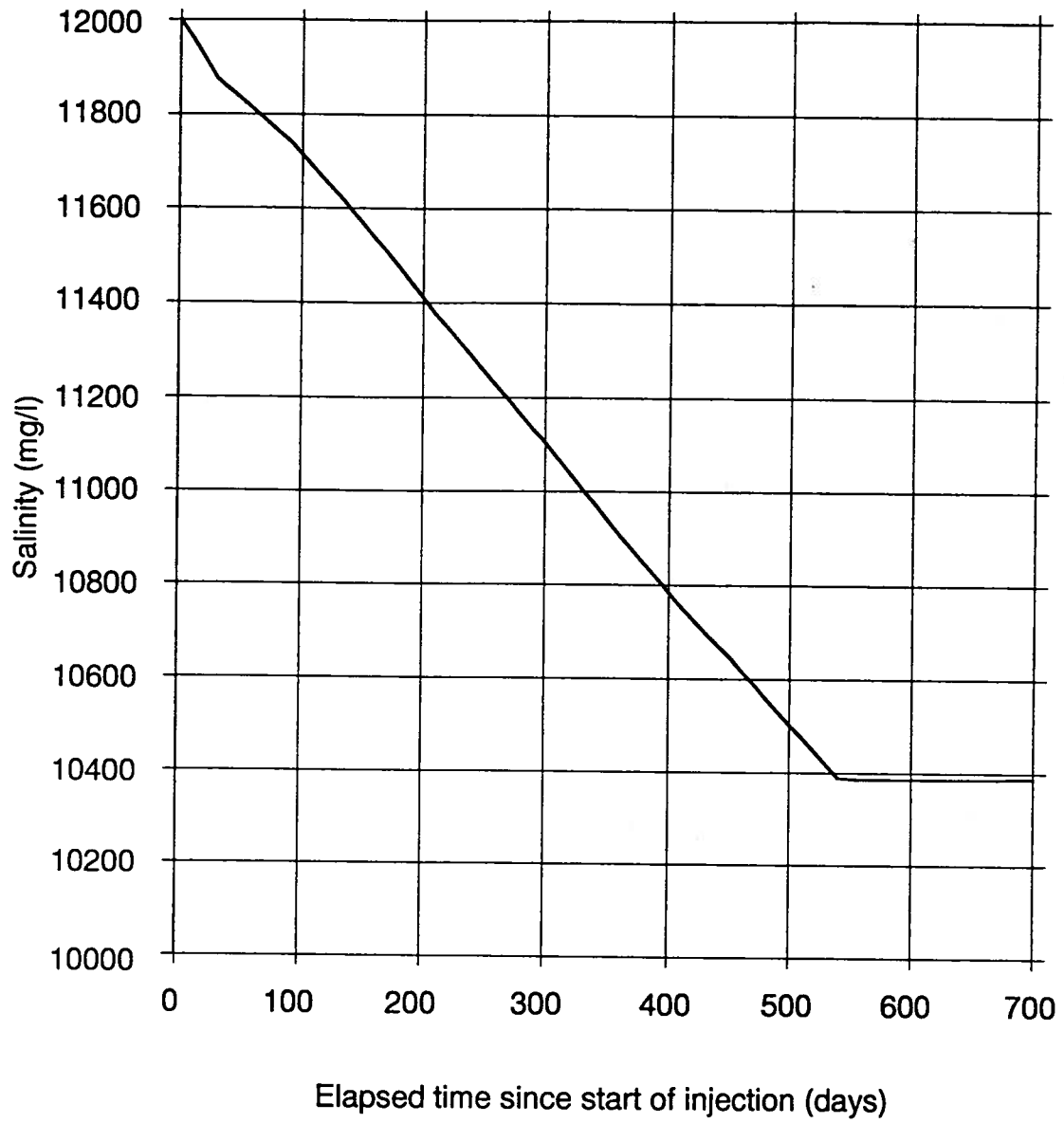


Figure 19: Calculated salinity decrease at the injection node in the Wabiskaw aquifer.



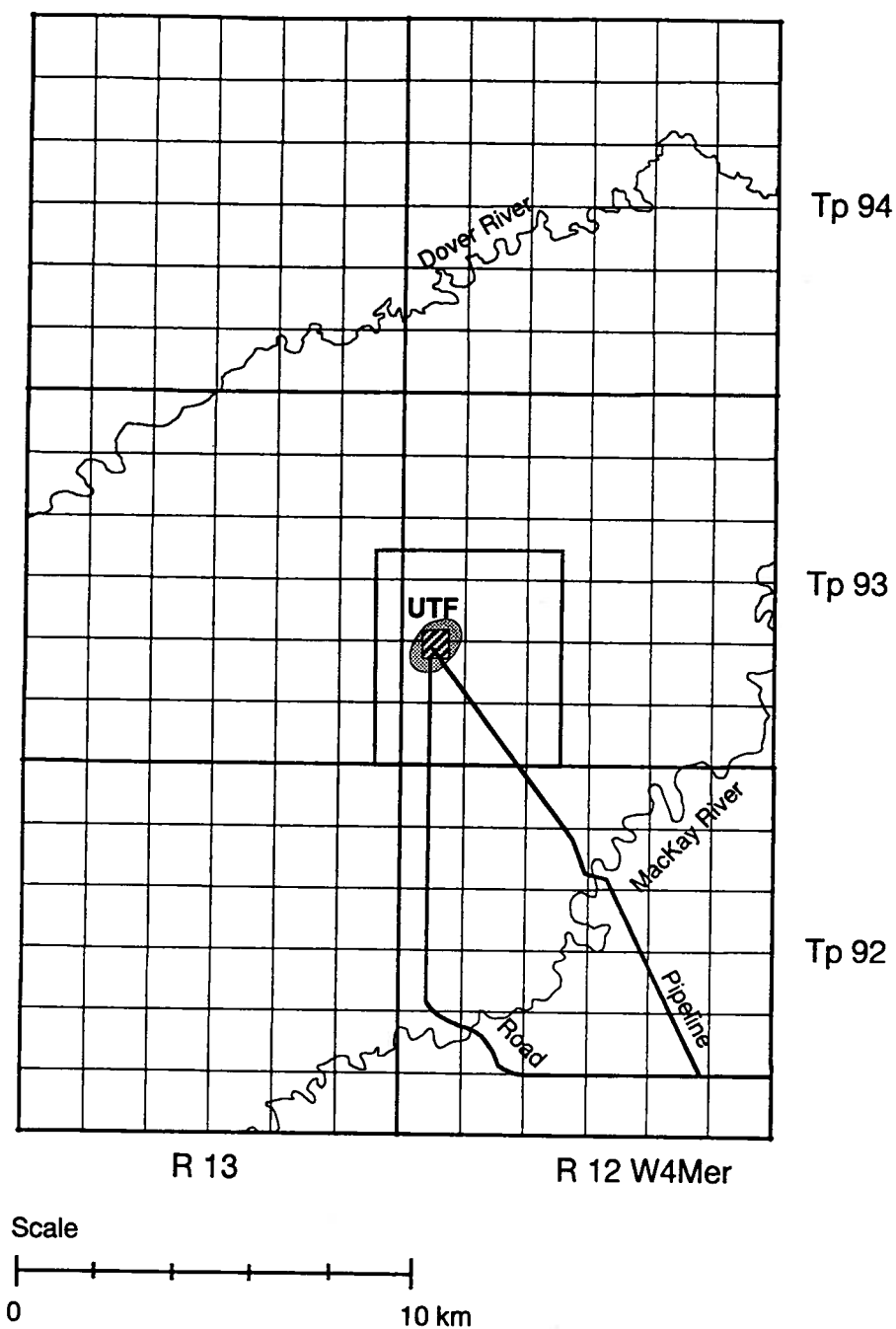


Figure 20: Calculated areal spread of the dilution plume in the Wabiskaw aquifer at the end of the injection period.

## CONCLUSIONS

Expansion of the AOSTRA Underground Test Facility operations requires disposal of residual water, to be achieved by injecting up to 900,000 m<sup>3</sup> over a period of two years into the Wabiskaw aquifer until a long term solution is found. The Wabiskaw aquifer is overlain by the Clearwater aquitard, which separates it from the protected shallow groundwater zone above it. In a previous preliminary assessment of the geochemical and hydrodynamic effects of injection it was established that the Wabiskaw aquifer is the only one at the site capable of accepting the proposed volume of injected residual water without reaching high pressures which may lead to rock fracturing. The assessment was based on numerical modelling of fluid flow in an aquifer assumed to have homogeneous properties. Also, geochemical modelling has shown that potential reactions between the injected water and aquifer water and rocks are likely to have negligible effects. The present study built on the previous results by concentrating on the hydrodynamic, thermal and salinity effects of injection in an aquifer of variable rock properties, particularly porosity. This continuation was dictated by the fact that the injected water has higher temperature and lower salinity than the aquifer water.

The porosity variation in the aquifer was determined based on geophysical logs calibrated on core analyses, thus increasing significantly the data base and areal coverage. Porosity varies between 15% and 32%, with an average of 24% (less than the value of 31% obtained previously from core analyses). The porosity distribution exhibits

an areal trend of lower values in the south-southeast of the UTF site, and higher values in the north. The permeability of the Wabiskaw aquifer is high, of the order of  $4 \times 10^{-12} \text{m}^2$  (4 darcies), leading to high hydraulic diffusivity.

The hydrodynamic, thermal and salinity effects of injection were studied using mathematical and computer modelling of coupled fluid flow, heat transfer and mass transport processes in porous media. The model takes also into account the compression of the pore space as a result of increased pressures (geomechanical effects). The simulations indicate that the pressure buildup at the injection site will closely follow the variation in the injection rate, remaining below the rock-fracturing threshold, and that it will rapidly decay after cessation of injection due to high aquifer hydraulic diffusivity. The pressure buildup around the injection site will likely be asymmetric, most probably due to the porosity distribution. At the end of the injection period, pressure buildup effects might be felt at up to 6 km southeast of the site, but only at up to 4 km away in the northwest. This pressure-buildup distribution correlates with low aquifer porosity in the southeast and high porosity in the north-northwest.

Unlike pressure, thermal effects are not likely to be felt far from the injection site, only at several hundred meters. This is because heat will be transferred from the higher temperature injected water to the low temperature aquifer water and rock. In addition, heat will be lost by conduction through the overlying and underlying shaley aquitards. After cessation of injection, the temperature at the injection site will slowly decrease

because heat transfer will take place by conduction only.

Because of lower salinity of the injected water, a dilution plume will form during injection. The spread of this plume will be driven mainly by advection induced by injection and by hydrodynamic dispersion in the porous aquifer rock. The injected water will mix with aquifer water, such that the dilution plume will have variable concentration, lower around the injection site and higher toward the edges. At cessation of injection, the edges of this plume will likely reach a distance of 300 - 500 m on average from the injection site. The plume will be slightly asymmetric, reaching up to 500 m in the northeast, and 350 m in other directions. This asymmetry is most likely due to the effect of the northeastward natural flow of aquifer water. Because of the rapid decay of the pressure buildup after cessation of injection, the dilution plume will be driven by the natural flow of aquifer water, whose velocity is estimated to be approximately 2.5 m/a. Under these circumstances, it will take over 1000 years for the dilution plume to reach discharge areas along the MacKay River.

In conclusion, numerical modelling of the hydrodynamic, thermal and salinity effects of injection at the UTF site indicate that, under the proposed injection scenario, these effects are not likely to affect in any significant way the integrity of the Wabiskaw aquifer and of any other formation or aquifer at the site.

## REFERENCES

- AOSTRA - Alberta Oil Sands Technology and Research Authority, (1992): Application to develop waste water disposal wells at the Underground Test Facility; Submitted to the Energy Resources Conservation Board.
- Bachu, S. (1993): Basement heat flow in the Western Canada Sedimentary Basin. *Tectonophysics*. v. 222, pp. 119-133.
- Bachu, S., (1991): On the effective thermal and hydraulic conductivity of binary heterogeneous sediments. *Tectonophysics*, v. 190, pp. 299-314.
- Bachu, S., and R.A. Burwash, (1991): Regional-scale analysis of the geothermal regime in the Western Canada Sedimentary Basin. *Geothermics*, v. 20(5/6), pp. 387-407.
- Bear, J. (1972): Dynamics of fluids in porous media. Elsevier, New York, 764 p.
- CPA - Canadian Petroleum Association, (1991): Production Waste Management Handbook for the Alberta Petroleum Industry, Calgary, Alberta.
- Domenico, P.A. and F.W. Schwartz, (1990): Physical and Chemical Hydrogeology; John Wiley & Sons, New York, 824 p.

- Gupta, S.K., C.R. Cole, F.W. Bond and A.M. Monti, (1984a). Finite-element three dimensional groundwater (FE3DGW) flow model formulation, program listings and users' manual; Pacific Northwest Laboratory, Richland, Washington.
- Gupta, S.K., C.R. Cole and G.F. Pinder, (1984b): A finite-element three-dimensional groundwater (FE3DGW) model for a multiaquifer system; Water Resources Research, v. 20, pp. 553-563.
- Gupta, K.S., C.R. Cole, C.T. Kincaid and A.M. Monti, (1987): Coupled Fluid, Energy, and Solute Transport (CFEST) Model: Formulation and User's Manual; Office of Nuclear Waste Isolation, Battelle Memorial Institute, Columbus, Ohio.
- Li, Y.H. and Gregory, S., (1974): Diffusion of ions in sea water and in deep-sea sediments; Geochimica and Cosmochimica Acta, v. 38, pp. 703-714.
- Marsily, G. de, (1986): Quantitative Hydrogeology; Academic Press, San Diego, 440 p.
- Nelson, L.R., Stevens, J.P. and Ksienski, N., (1991): Disposal of produced water at in situ pilot operations in Athabasca; Proceedings of the Environmental Committee Meeting of the Canadian Heavy Oil Association on "Water Management of Heavy Oil Operations", Calgary, November 12, 1991.
- Petroleum Geology and Basin Analysis Group, (1992): Baseline Hydrogeologic al regime at the intermediate scale, AOSTRA Underground Test Facility; report to Environment Canada, Conservation and Protection, 134 p.

**Petroleum Geoscience Section, (1993): Preliminary evaluation of geochemical and hydrodynamic effects of deep injection of residual water at the AOSTRA Underground Test Facility; report to Environment Canada, Conservation and Protection, 97 p.**

**Sadler, K.W., (1991): A regulatory perspective on water management for oil sands operations; Proceedings of the Environmental Committee Meeting of the Canadian Heavy Oil Association on "Water Management of Heavy Oil Operations", Calgary. Nov. 12, 1991.**